



**INLAND WATERS BRANCH**

**DEPARTMENT OF ENERGY, MINES AND RESOURCES**

*Regional Groundwater Flow  
between Lake Simcoe and Lake Ontario*

C. J. HAEFELI

TECHNICAL BULLETIN NO.23



CANADA

TECHNICAL BULLETIN NO.23

*Regional Groundwater Flow  
between Lake Simcoe and Lake Ontario*

C. J. HAEFELI

INLAND WATERS BRANCH  
DEPARTMENT OF ENERGY, MINES AND RESOURCES  
OTTAWA, CANADA, 1970

# Contents

	Page
ACKNOWLEDGEMENTS. . . . .	v
PREFACE . . . . .	vii
CHAPTER 1. INTRODUCTION. . . . .	1
CHAPTER 2. HYDROGEOLOGICAL PROPERTIES OF QUATERNARY DEPOSITS . . . . .	4
CHAPTER 3. INTERPRETATION OF REGIONAL GROUNDWATER FLOW . . . . .	9
CHAPTER 4. CONCLUSIONS . . . . .	38
REFERENCES. . . . .	39

## Illustrations

Figure 1. Index map . . . . .	viii
Figure 2. Topography of study area. . . . .	1
Figure 3. Bedrock geology of study area . . . . .	2
Figure 4. Composition of the quaternary deposits (after drillers' logs) . . . . .	4
Figure 5. Cumulative curves for the specific capacity of overburden wells > 200 feet. 217 wells of the entire area and 88 wells of the main channel area . . . . .	5
Figure 6. Time/drawdown curve of a water well and an observation well at Markham (York Co.), Dec. 1964 . . . . .	6
Figure 7. Time/drawdown curve of an observation well (York Co., Vaughan Twp.), May 1966 . . . . .	7
Figure 8. Time/drawdown curve of an observation well at Richmond Hill, April 1963. . . . .	8
Figure 9. Time/drawdown curve of an observation well at Bradford (York Co., King Twp.), 1968 . . . . .	9
Figure 10. General piezometric surface established from deep wells drilled in the overburden covering the Upper Ordovician (shale) . . . . .	10
Figure 11. Cumulative curves for the specific capacity of 116 wells of Prince Edward Co. and 91 wells of Mariposa, Thorah and Brock Twps. drilled in the Coburg formation . . . . .	11
Figure 12. Approximate direction of groundwater flow in the Middle Ordovician limestone. . . . .	12

## *Illustrations (Cont'd)*

	Page
Figure 13. Surface elevation and piezometric head of wells reaching below the level of Lake Simcoe. . . . .	13
Figure 14. Distribution of piezometric head and percentage of flowing wells versus well depth in area I south of Lake Simcoe. . . . .	14
Figure 15. Distribution of flowing and artesian wells between area I and area II south of Lake Simcoe. . . . .	14
Figure 16. Schematic presentation of well groups of area I, area II, and area > 850 ft. a.s.l. south of Lake Simcoe. . . . .	15
Figure 17. Distance from the basin boundary versus conductivity. . . . .	21
Figure 18. Distance from the basin boundary versus chloride content. . . . .	22
Figure 19. Chemical analysis of group 1: Wells located within 6 miles of the basin divide . . . . .	24
Figure 20. Chemical analysis of group 2: Wells located 6 - 21 miles from the basin divide . . . . .	25
Figure 21. Base exchange index versus distance from basin divide . . . . .	27
Figure 22. Computation of the saturation point $S_0$ of $CaSO_4$ . . . . .	30
Figure 23. Computation of pH of equilibrium and saturation index . . . . .	32
Figure 24. Saturation point of $CaCO_3$ , $k_r$ as function of the ionic strength (after H. Schoeller: 1962, 279) . . . . .	32
Figure 25. Bedrock topography between Lake Simcoe and Lake Ontario (with contribution from G.D. Hobson, Geol. Surv. of Canada) . . . . .	36
Plate I. Hydrogeological cross sections between Lake Simcoe and Lake Ontario . . . . .	Inside back cover
Plate II. Simulated groundwater flow between Lake Simcoe and Lake Ontario. . . . .	Inside back cover

## *Acknowledgements*

The author would like to express his gratitude to his colleagues, and the summer assistants and cooperating agencies who made this study possible. My sincere thanks go to:

Douglas French, Kevin Coombs, and Ronald Crosby, who provided outstanding field assistance during the summer 1969.

George Hobson, Hugh McAuley, and Robert Gagné, of the Geological Survey of Canada, for their bedrock surface map, included in this report.

Jean Charron, for the interesting and stimulating discussions in groundwater hydrochemistry.

Allan Freeze, for the enlightenment provided by his comments in the field of regional groundwater flow.

Myles Parsons and Robert van Everdingen, for their competent and critical review of the manuscript.

Jack Kirk, International Water Supply Ltd., Oakville, who provided additional well records to complete our survey.

Officials of the Water Quality Division of the Inland Waters Branch for the chemical analysis of the collected water samples.

## *Preface*

Lake Ontario and its drainage basin has been selected as the type area to investigate for the International Field Year on the Great Lakes (IFYGL). The IFYGL is co-sponsored by the Canadian and United States National Committees for the International Hydrological Decade (IHD). The terrestrial water balance is one of the four inter-disciplinary program areas, and its objective is to determine the total inflow to and outflow from the lake.

This paper is a part of the project "Groundwater Inflow into Lake Ontario" (IHD - Project GW68-3). It examines the particular hydrogeological conditions north of Toronto in an attempt to determine if the terrestrial water balance of the Lake Ontario Basin is affected by major seepage from Lake Simcoe.

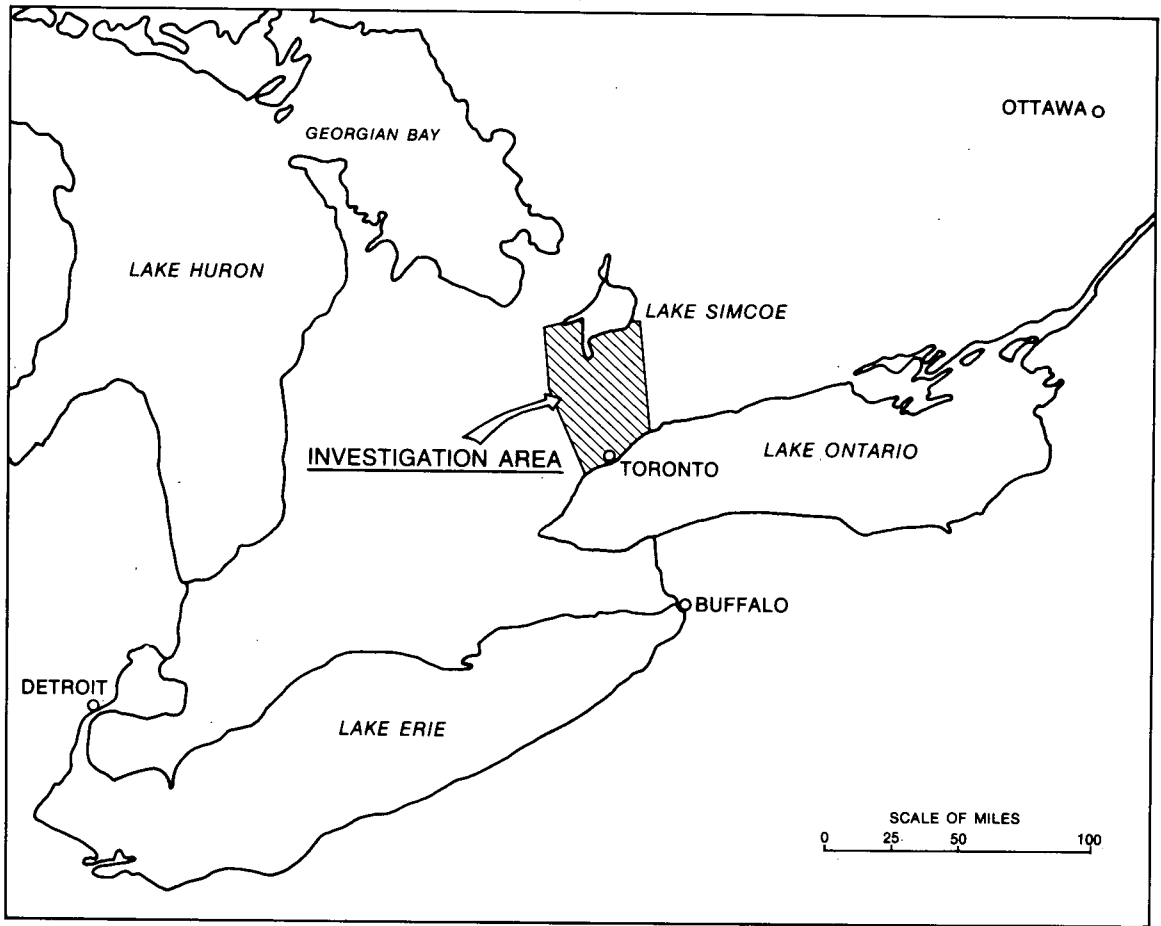


Figure 1. Index map.

## Introduction

Lake Simcoe is 35 to 40 miles north of and about 470 feet higher than Lake Ontario. However, the average elevation of the Lake Simcoe Basin is only about 250 feet higher. The surface water divide within the study area of 600 square miles lies mainly between elevations 900 and 1100 feet. The general topography, the main drainage features and the basin boundaries are shown in Figure 2.

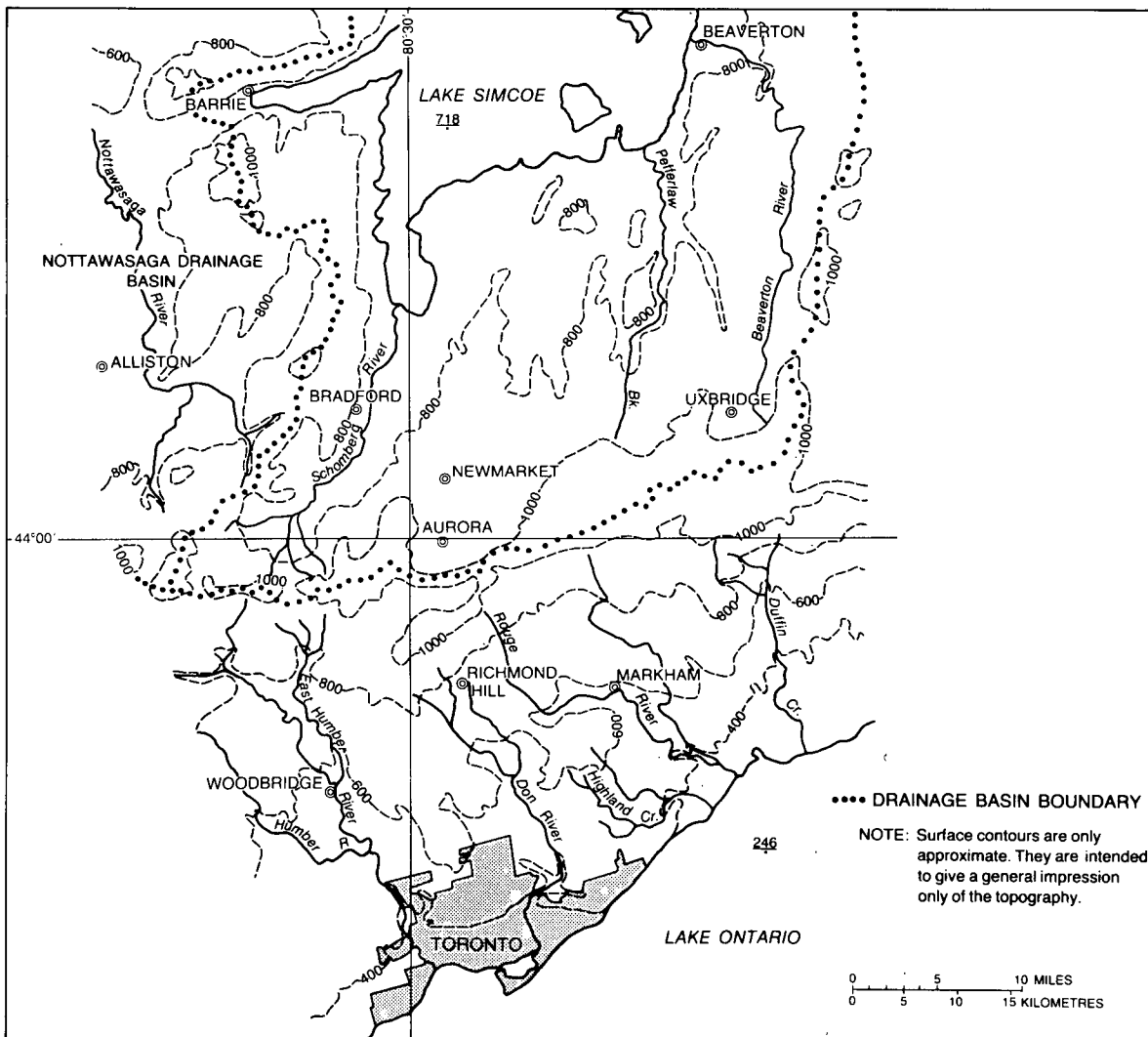


Figure 2. Topography of study area.



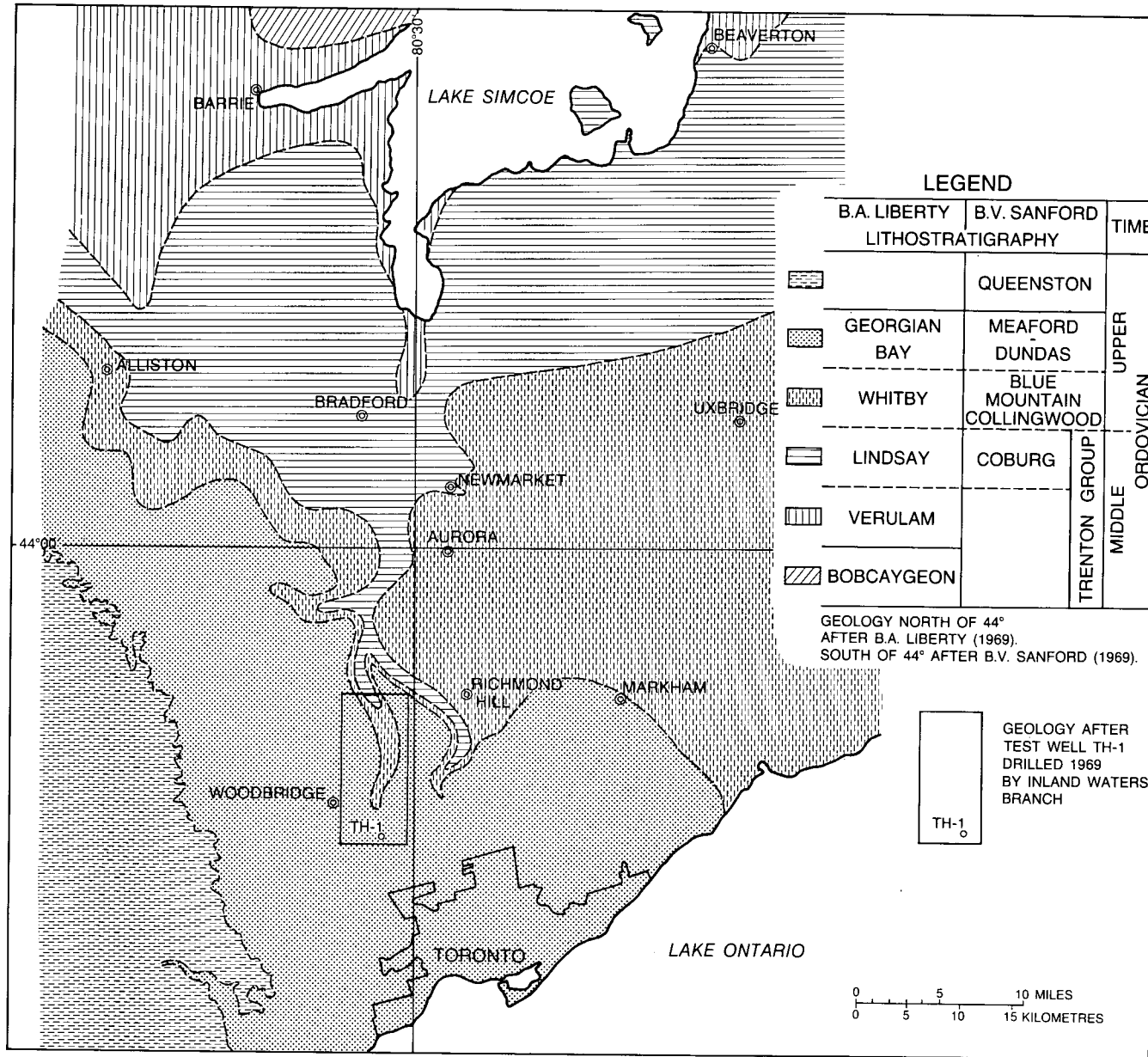


Figure 3. Bedrock geology of study area.

The east-west directed drainage divide is composed of a till and kame moraine, the Oakridges moraine, which was formed during the recession of the Wisconsin Glacier in the later Pleistocene in the course of a re-advancement of its Ontario and Northern Lobe (Deane, 1950, p. 85; Chapman and Putnam, 1949, p. 23). Most of the Lake Simcoe lowlands are covered with ground moraine material and drumlins. South of the Lake Simcoe shore and along the Nottawasaga Valley, large belts are floored by glacio-lacustrine sediments, mainly sand. Swamps and bogs occur in the Schomberg and Pefferlaw valleys and are scattered over the whole lowlands, especially in the eastern part. South of the Oakridges moraine, Chapman and Putnam (1966) recognized, from north to south, three physiographic units: 1) the South Slope, consisting mainly of till, 2) the Peel Clay Plain, its central part, and 3) the Iroquois Plains, the lowlands bordering Lake Ontario which were inundated late in the Pleistocene age by Lake Iroquois. Drumlins are scattered over the area, especially between Richmond Hill and West Hill. Along the shore at Scarborough the erosion has cut into till and clay of Pleistocene age, forming the steep 200- to 350-foot high Scarborough Bluffs. During preglacial times the drainage coming from the upper Great Lakes area passed through the Georgian Bay depression and continued directly to the Lake Ontario basin (Chapman and Putnam, 1949, p. 11), eroding channels in the bedrock. These valleys have probably been reshaped during the following glacial period(s), and are buried now by glacial and fluvio-glacial deposits sometimes over 600-feet thick. They were first indicated by oil, gas, and water wells (Deane, 1950; Watt, 1957).

The entire area is underlain by sedimentary formations of the Ordovician system (Figure 3) which lie upon the eroded surface of the Precambrian or Canadian Shield. The Upper Ordovician is composed mainly of shale with minor interbeds of siltstone, limestone and dolomite in the upper part (Queenston, Meaford-Dundas formations) whereas the lower part consists of dark, mostly bituminous, shale (Blue Mountain, Collingwood formations). The Middle Ordovician is formed by the Trenton Group which is essentially composed of limestone. A sequence of grey-brown, microcrystalline limestone represents the Coburg formation. The lower part (Verulam, Bobcaygeon formations) consists of microcrystalline, calcarenite, argillaceous limestone with shale interbeds.

Since the whole study area is covered with thick quaternary deposits, bedrock outcrops are very scarce. The structure of the bedrock has therefore to be evaluated from oil and gas well records, and features observed in other areas. The inclination of the flat bedding is approximately  $0.20^{\circ}$  -  $0.30^{\circ}$  S to SSW. Other than the Algonquin Arch, which produces a very wide, slightly anticlinal structure west of Lake Simcoe, and the Peterborough Arch outside the study area, no major structures have been reported (Liberty, 1969, p. 86). The irregular formation boundaries are mainly caused by the eroded bedrock surface. They give an impression of the bedrock relief which is particularly strong in the area of Richmond Hill, showing major channels.

The relatively high elevation of the Lake Simcoe Basin, the south dipping surface and bedding of the bedrock, and especially the north-south directed, deep bedrock channels point to the possible existence of a south-bound groundwater flow system.

## *Hydrogeological Properties of the Quaternary Deposits*

A survey of wells within the study area was made to obtain hydrologic information about the overburden. The water-well data were taken from all available Ground Water Bulletins published by the Ontario Water Resources Commission (1953-1959). Oil and gas well logs were obtained from records of the Department of Energy and Resources Management of Ontario (1880-1967).

A map plot of drillers' lithologic logs was made using some 200 wells (minimum depth of 200 feet) producing cross-sections through the overburden which showed two main features:

a) The drift thickness varies considerably (compare Figure 2 with Figure 25, Plate 1). Apart from the well defined bedrock channels the following trend can be observed. From less than 50 feet at the southeastern shore of Lake Simcoe, the overburden increases to over 400 feet in the area between Newmarket and Richmond Hill. There it begins to decrease southwards becoming 25 - 75 feet thick along Lake Ontario's shoreline south and west of Toronto. An east-west section shows the largest accumulation in the central part, a distinct decrease to 150 feet and less in the area of Woodbridge, and a variable thickness around Markham of 100 - 250 feet.

b) Regional, extensive, well defined aquifers do not exist. The general pattern of the quaternary deposits takes the form of a body of very low permeability, with enclosed high permeable lenses of various sizes. Figure 4

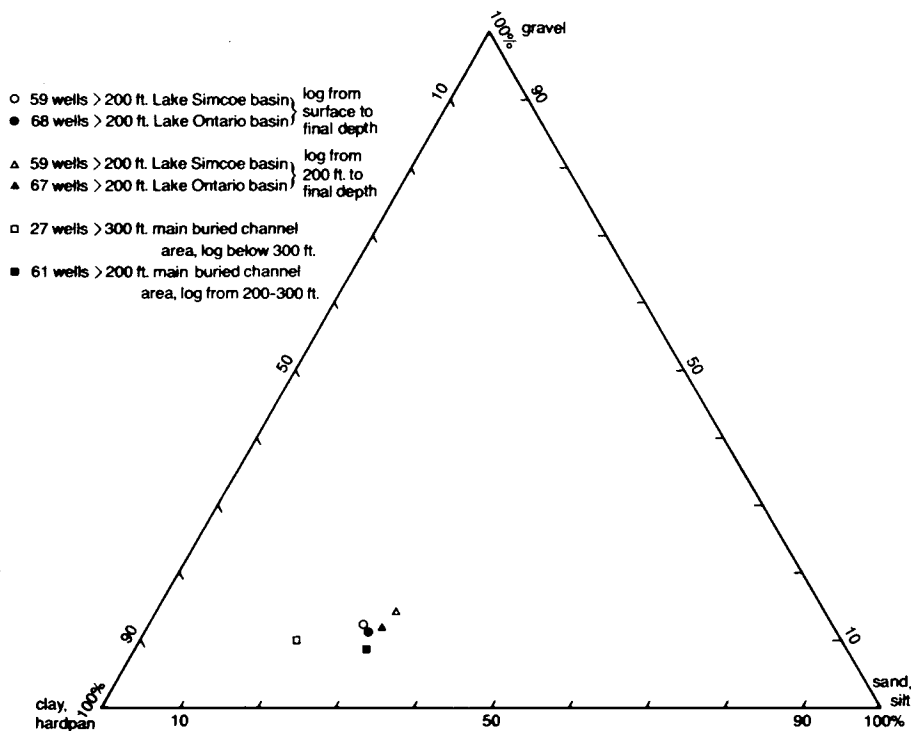


Figure 4. Composition of the quaternary deposits (after drillers' logs).

shows the overall composition of the overburden for various ranges of depth in both basins as well as for the main channel area connecting Cook Bay and Humber Bay. The composition is almost identical in all groups except the deepest part of the channel. The lithologic terms of Figure 4 were taken from the drillers' logs but do not necessarily correspond with their lithologic meaning. For example, many drillers will consider silt to be sand or quicksand, and gravel might even represent a till, showing the strata to be generally more permeable than it really is. Taking this into account, it is safe to say that over 2/3 of the overburden has a very low permeability and less than 1/6 has a permeability which makes it suitable for aquifer material.

The specific capacity,  $Q/s$ , was computed for 217 wells spread over the whole region, and for 88 wells within the main channel area (minimum well depth of 200 feet). The result is given as a cumulative curve in Figure 5. Both curves show the consequences of the lithologic composition (Figure 4). The channel area gives a slightly less favourable picture. More than half of the wells produced less than 0.1 l gpm/ft and only 19 per cent or 13 per cent had a specific capacity of over 1.0. The generally poor production of the deeper drift layers and the limited yield common to small aquifers with little recharge again indicates the nonexistence of well defined, extensive aquifers.

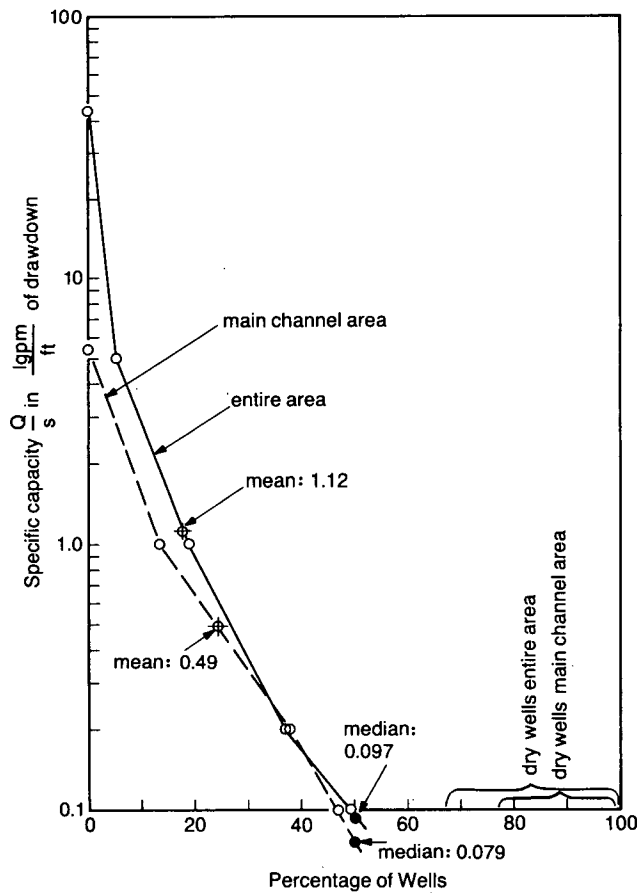


Figure 5. Cumulative curves for the specific capacity of overburden wells > 200 feet. 217 wells of the entire area and 88 wells of the main channel area.

To show some quantitative properties of the highest permeable overburden lenses, existing pumping test data, considered to be characteristic of the study area, were evaluated. The wells were constructed after 1960 for industrial or municipal water supplies. All are exploiting confined aquifers at various depths (67 - 385 feet), and have a piezometric head close to the surface (-16 feet to flowing). The time/drawdown curves of the observation wells show in three of four examples (Figures 6 to 9) impermeable boundary conditions, typical of the very inhomogeneous overburden. After a short time of pumping the cone of depression reaches a poor permeable boundary and the flow to the well starts to decrease. At this point the data plot deviates from the nonequilibrium Theis type curve, indicating the shortage of supply. Since all tests were performed in populated areas, it is possible that the departures of the data plot might have been partially caused by nearby pumped wells. Therefore, a computation of the distance between the wells and the impermeable boundaries by applying the image well theory was not attempted. Impermeable boundary conditions are observed in most of the pumping tests in this region. The transmissibility values,  $T$ , of the four examples ranging from 40,000 - 83,000 Igpd/ft are considered among the highest of our study area. The mean of the entire overburden is in the order of 2000 - 3000 Igpd/ft, as calculated from  $Q/s$  after the method of Meyer (1963, p. 339). The storage coefficient,  $S$ , of the plotted pumping tests shows the characteristic low values for confined conditions.

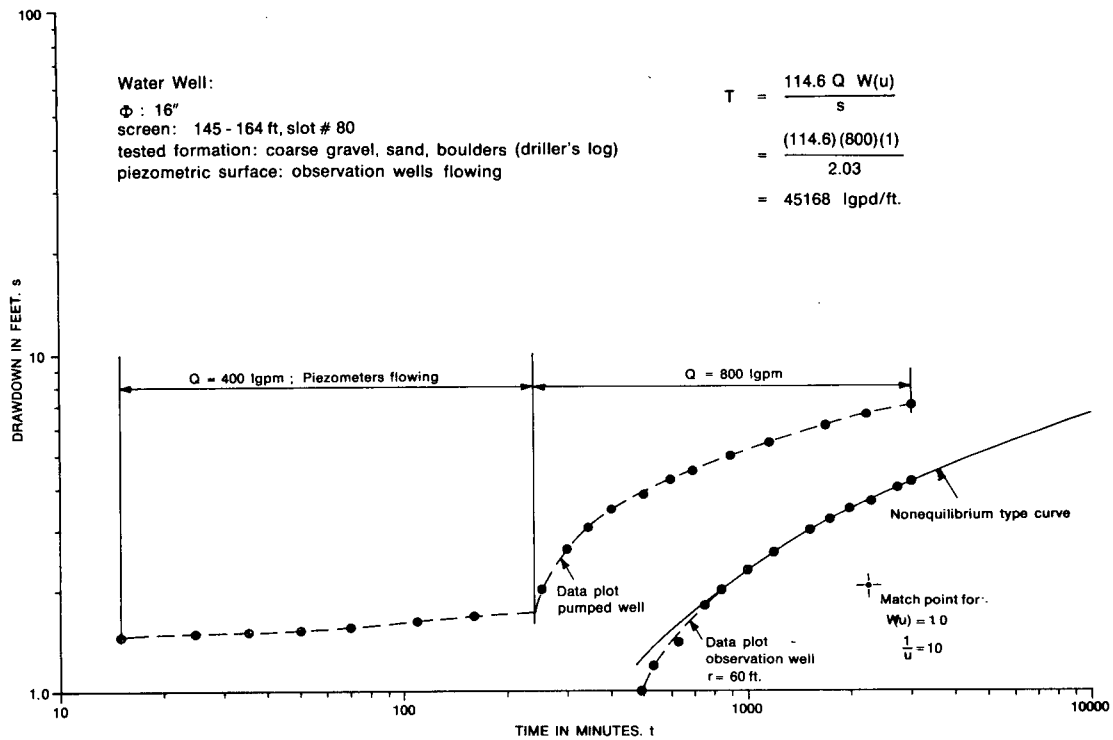


Figure 6. Time/drawdown curve of a water well and an observation well at Markham (York Co.), Dec. 1964.

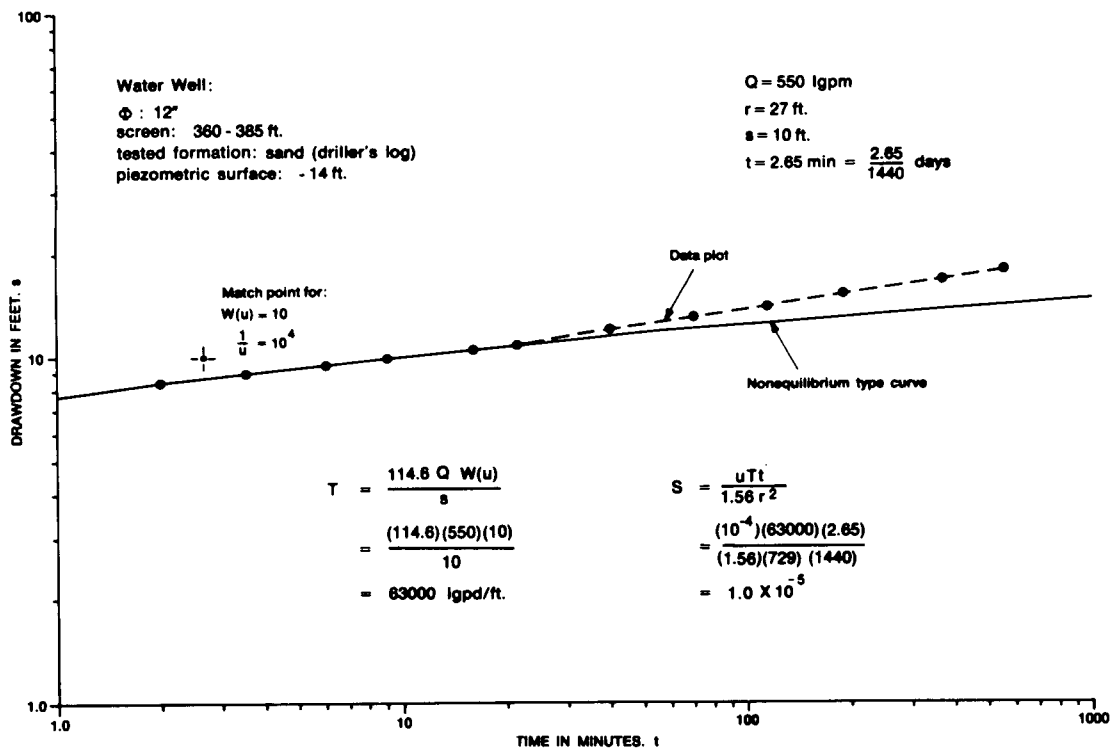


Figure 7. Time/drawdown curve of an observation well (York Co., Vaughan Twp.), May 1966.

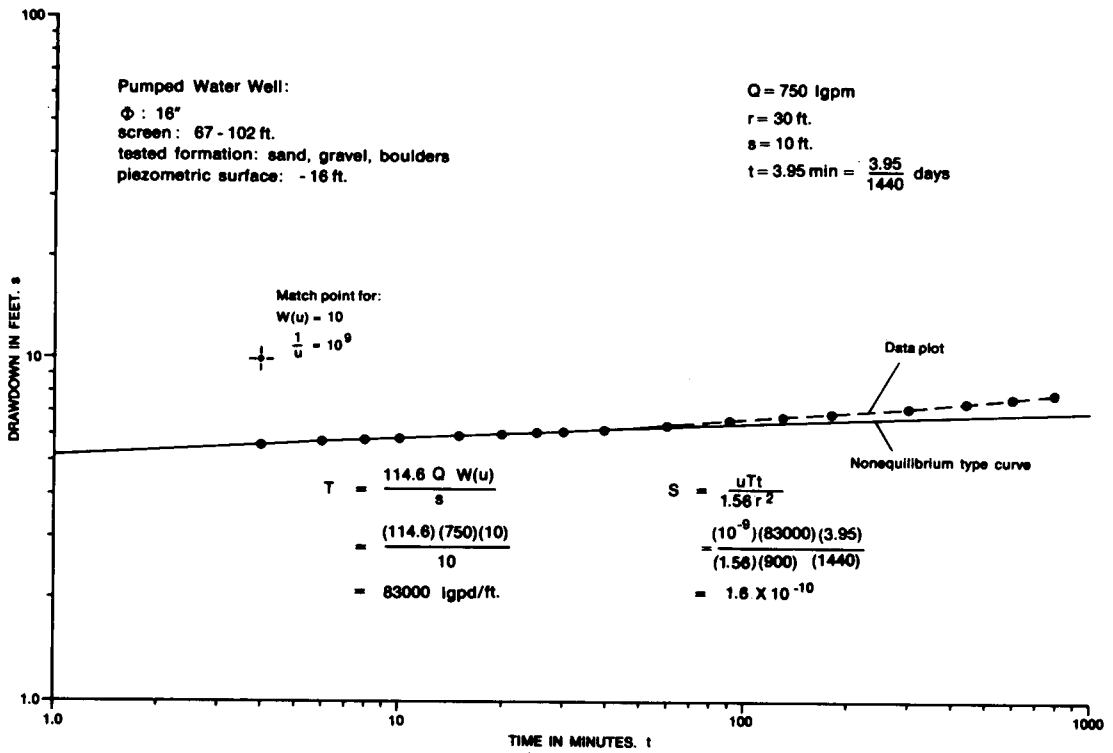


Figure 8. Time/drawdown curve of an observation well at Richmond Hill, April 1963.

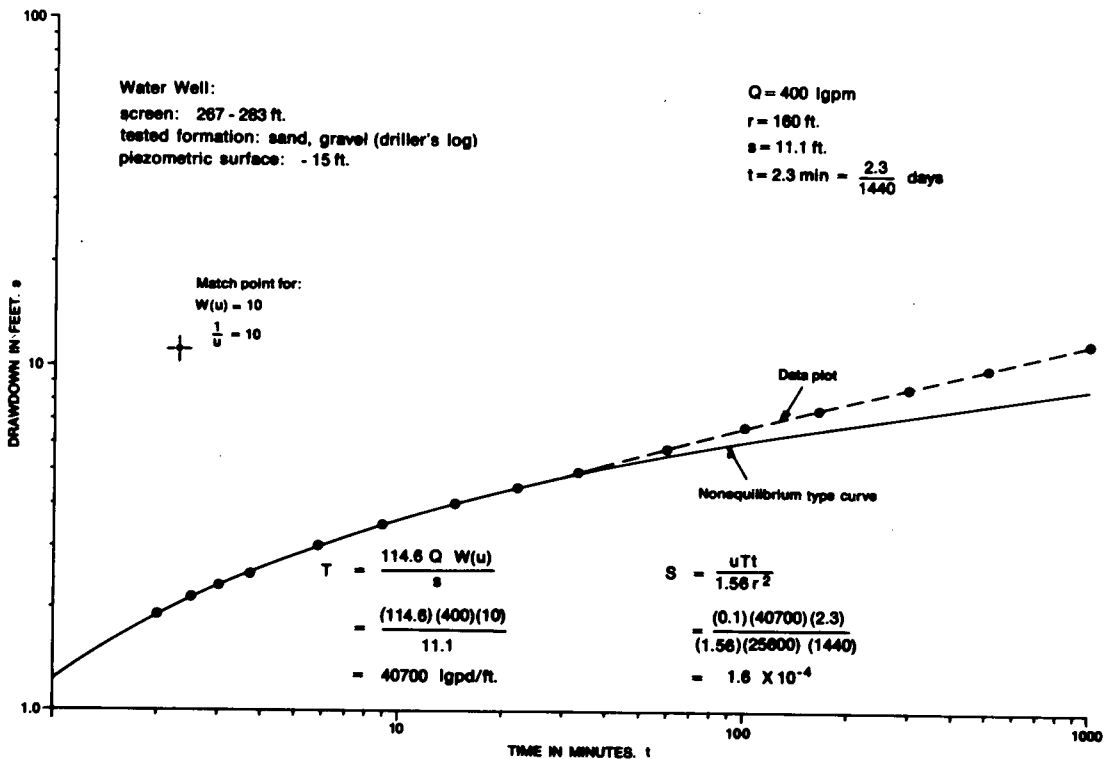


Figure 9. Time/drawdown curve of an observation well at Bradford (York Co., King twp.), 1968.

## *Interpretation of Regional Groundwater Flow*

To investigate the main groundwater flow systems in the study area, the following three independent tools were used:

- 1) Piezometric analysis
- 2) Hydrogeochemistry
- 3) Mathematical analysis

### PIEZOMETRIC ANALYSIS

The static water level or piezometric head of the existing wells was interpreted in two ways. To outline the flow pattern, two factors were analysed: a) the configuration of the water table, and b) the distribution of the hydraulic head south of Lake Simcoe.

#### a) Configuration of the Piezometric Surface

Water levels of shallow wells are assumed to be influenced by highly transient surface phenomena and therefore are not useful for study of the characteristics of relatively deep flow systems. For this reason a field survey of some 40 wells deeper than 200 feet, and distributed over the entire area was made. To fill area gaps, data of some inaccessible wells were taken from the well records. The depth limits of 200 feet and 300 feet were chosen to obtain a sufficient number of deep wells representing the hydraulic conditions in the vicinity of the bedrock. Despite limited reliable well data it was possible to outline the shape of the piezometric surface. The groundwater divide appears to have the same general direction as the morphologic boundary (Figure 10).

The direction of the groundwater flow in the Middle Ordovician limestone was also investigated. The main part of southern and southeastern Lake Simcoe is underlain by the Coburg formation. At Pefferlaw Creek and at the Georgian and Thorah Islands the limestone is outcropping, and is covered in other areas by rather shallow overburden layers. The Coburg formation consists mainly of grey to brown, microcrystalline limestone in beds that are 0.1 - 2.0 feet thick. In the Lake Simcoe area, Liberty (1969, p. 58) also observed shale partings along bedding planes and interbeddings of a few beds with 8- to 12-inch thick medium-crystalline, crinoidal limestone and calcarenite. The porosity of this generally dense rock is probably near 5 per cent and consequently the intergranular permeability is extremely low. Thus, if any exploitable groundwater exists in the formation there has to exist a groundwater movement through fractures. Unfortunately, there are not enough limestone wells south of Lake Simcoe to compute the magnitude of the permeability. Under the assumption that there is no considerable change in the distribution, spacing, and opening of the fractures and joints in the flat bedded limestone, data from outside the study area were applied. The specific capacity,  $Q/s$ , was computed for 117 limestone wells of Prince Edward County and 77 wells of Thorah, Brock and Mariposa townships (Ontario County) east of Lake Simcoe. The results are represented as cumulative curves (Figure 11) and show values not too different from those of the quaternary deposits (Figure 5). The Coburg formation therefore is an aquifer.



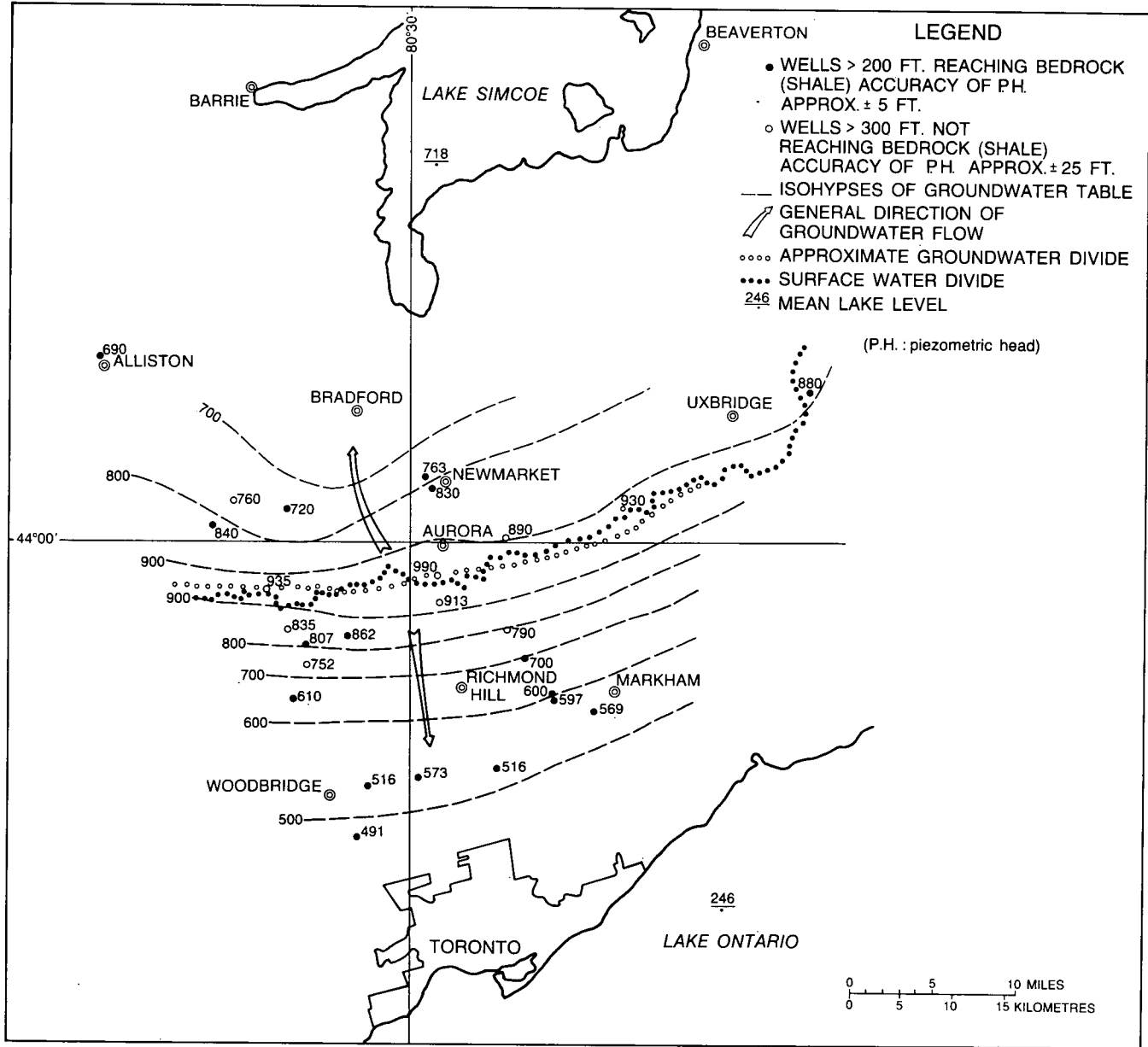


Figure 10. General piezometric surface established from deep wells drilled in the overburden covering the Upper Ordovician (shale).

All but three of the surveyed wells in the area of the Middle Ordovician limestone showed a higher hydraulic head than the mean level of Lake Simcoe, indicating that no important recharge, if any at all, occurs from the lake into the limestone or the overlying drift (Figure 12). Only one well near Alliston, which is in the Nottawasaga Bay basin, has a substantially lower piezometric head than the lake. The heads of two other wells bordering Lake Simcoe are close to the lake level but inside the tolerance margin. Five wells show artesian conditions; their piezometric level is not known, and the surface elevation (+) was marked instead. Despite the rather scarce distribution of wells, one can speculate on a general groundwater flow direction towards Lake Simcoe.

b) Distribution of Hydraulic Head

In a groundwater body, the hydraulic potential of a single flow system generally varies according to depth. In the discharge area, the hydraulic potential increases with depth; in the recharge area, the opposite is true. For example in the discharge area when the two piezometers are installed beside each other but at different depths, the water level in the deeper piezometer will be higher than that of the shallower one. The flow pattern in a specified area can therefore be evaluated by using water wells as piezometers and static water levels as piezometer heads measured with respect to a suitable datum.

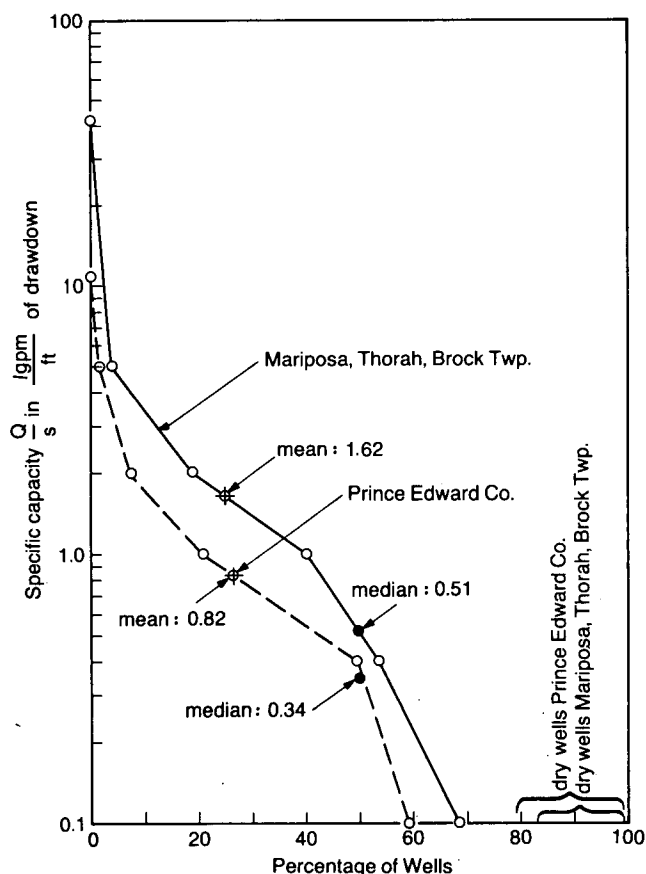


Figure 11. Cumulative curves for the specific capacity of 116 wells of Prince Edward Co. and 91 wells of Mariposa, Thorah and Brock Twp. drilled in the Coburg formation.

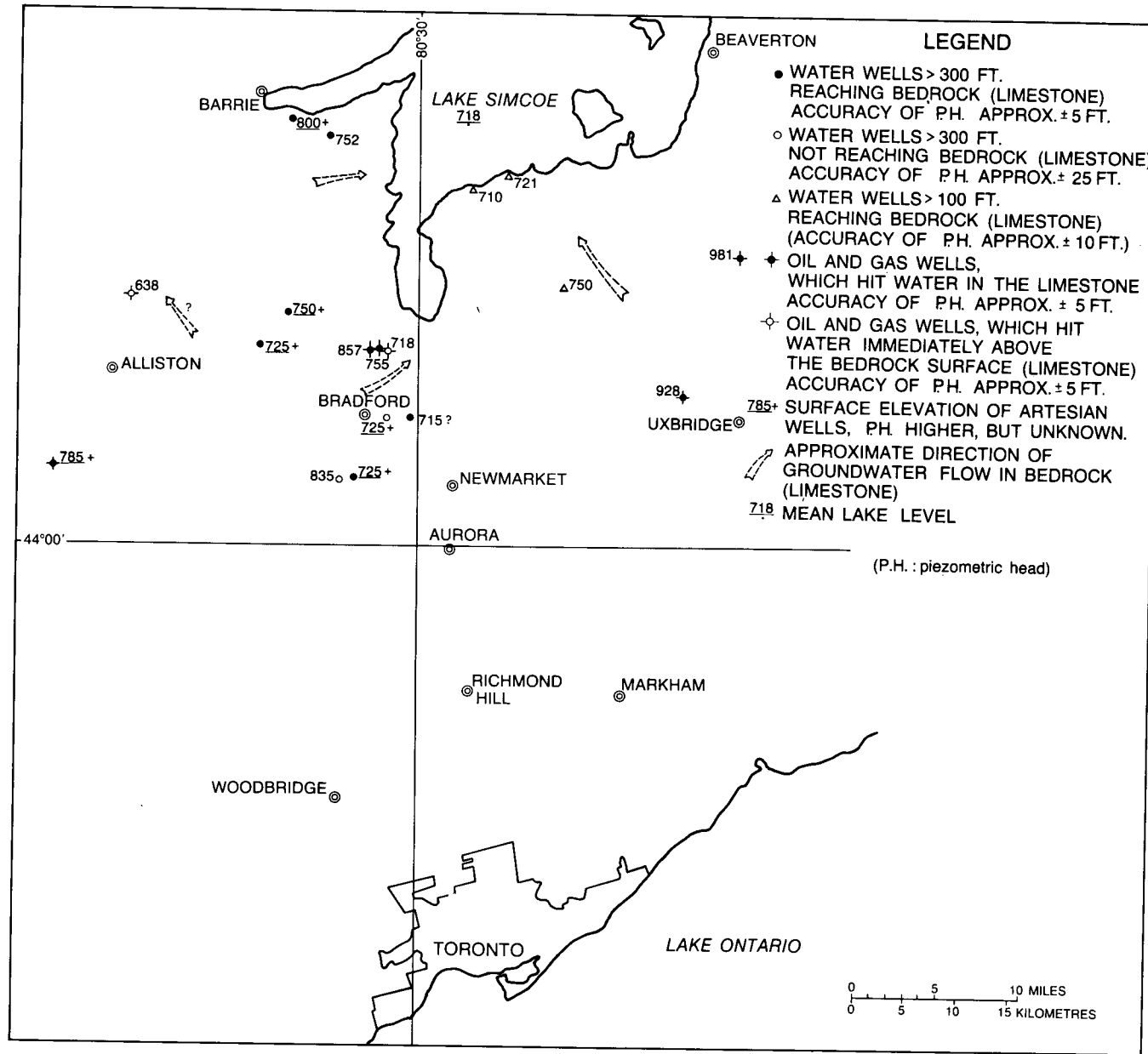


Figure 12. Approximate direction of groundwater flow in the Middle Ordovician limestone.

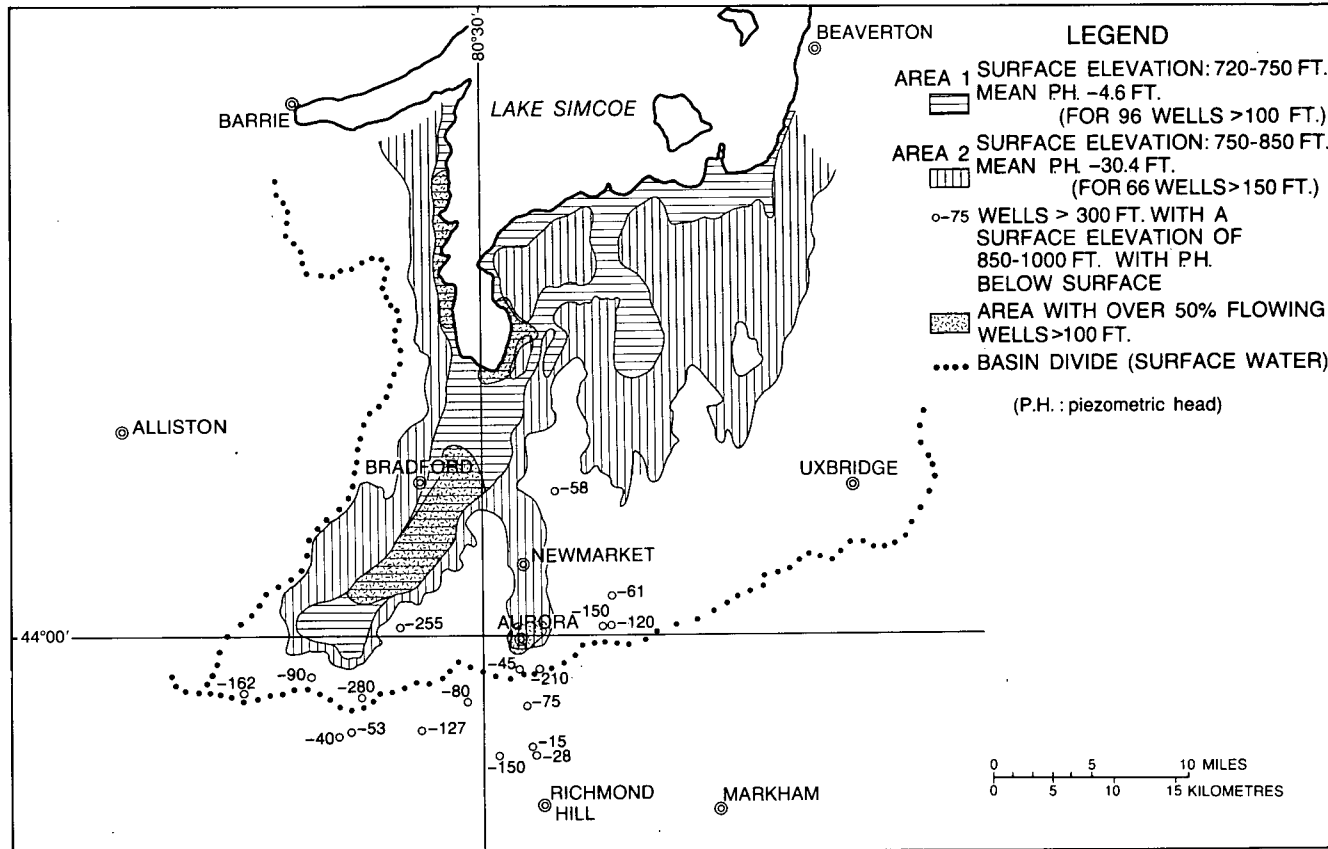


Figure 13. Surface elevation and piezometric head of wells reaching below the level of Lake Simcoe.

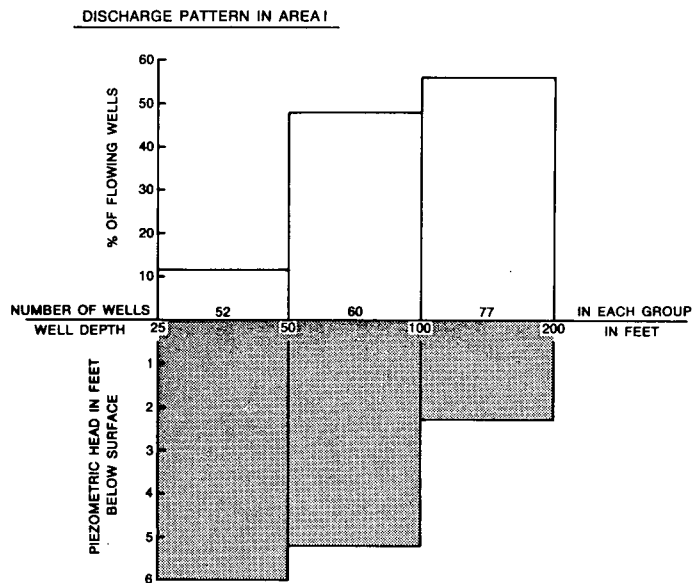


Figure 14. Distribution of piezometric head and percentage of flowing wells versus well depth in area I south of Lake Simcoe.

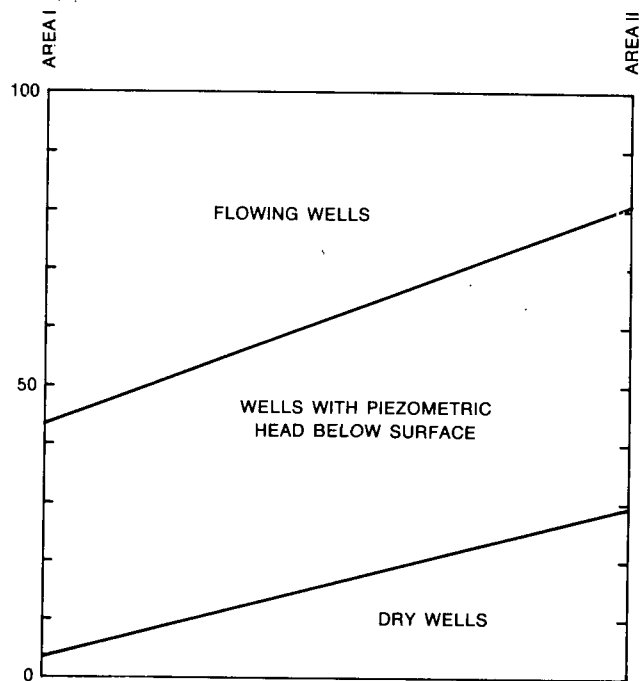


Figure 15. Distribution of flowing and artesian wells between area I and area II south of Lake Simcoe.

To verify the nature of flow immediately south of Lake Simcoe, the relationship between 189 wells was analyzed. The wells, situated in area I (Figure 13), had depths ranging from 25 to 200 feet and surface elevations of 720 - 750 feet. (Since exact well elevations and use of screens were not known, this very large number of wells was chosen to reduce the effect of

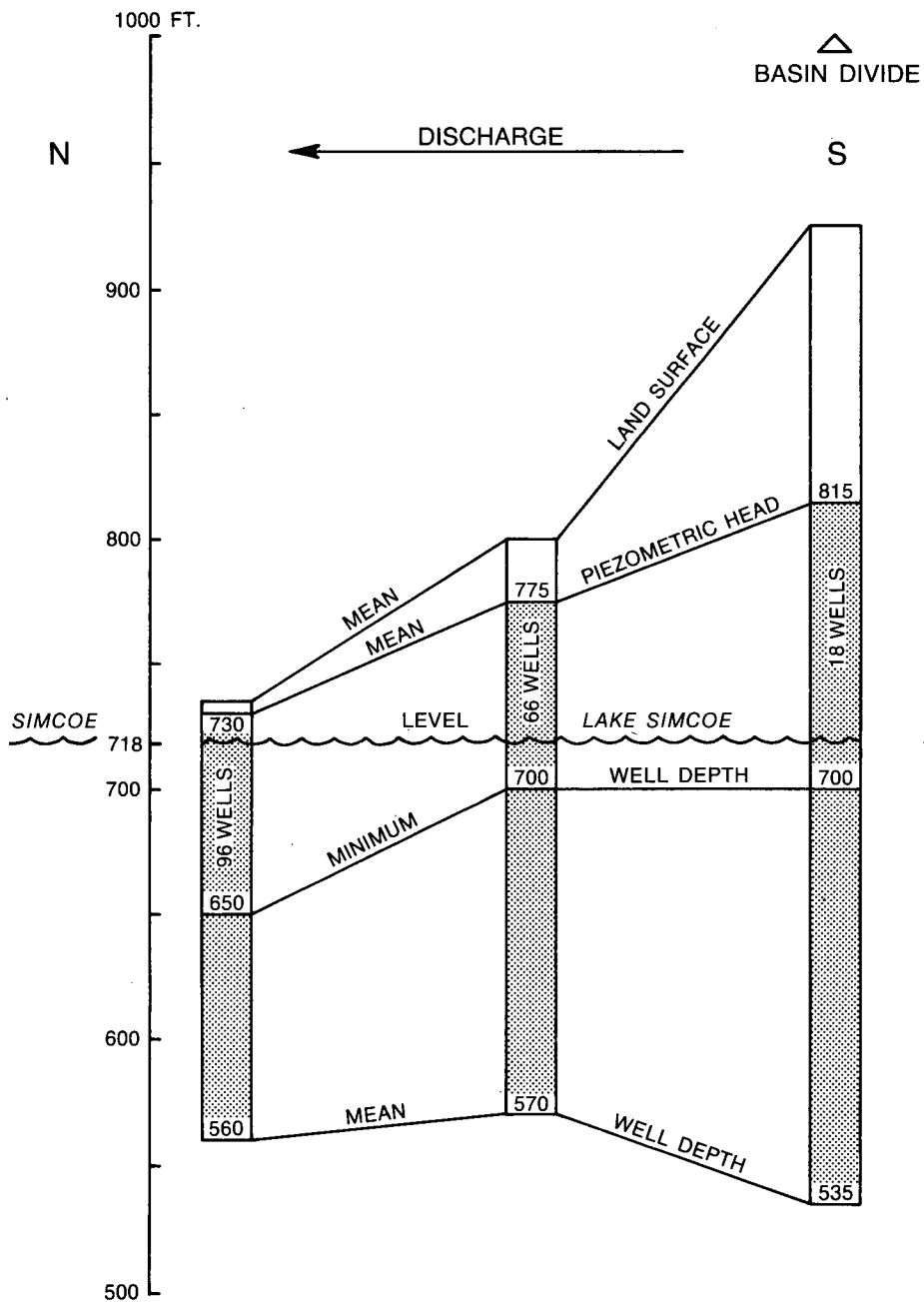


Figure 16. Schematic presentation of well groups of area I, area II, and area > 850 ft. a.s.l. south of Lake Simcoe.

any errors.) The result clearly showed discharge in area 1 (Figure 14). With the increasing hydraulic head of the deeper well groups the percentage of flowing wells increases. Since the levels of the artesian wells were not known, the rather arbitrary figure of +2 feet was assumed for all of them. The hydraulic head increases in area 1 by up to 2.5 per cent of the well depth difference. By comparing the percentage of flowing and dry wells reaching below lake level for different areas (Figures 13 and 15) the north-bound groundwater flow becomes apparent again. By checking the piezometric head of three different deep well groups, classified according to their surface elevation, the trend remains (Figures 13 and 16).

#### HYDROGEOCHEMISTRY

Water samples from most of the surveyed wells were taken for chemical analysis. The analyses were made by the Branch's Water Quality Division. Out of a total of 30 samples, 11 had to be rejected either because of high nitrate content or because the producing aquifer was too shallow. According to Thomas (1953, p. 59) most nitrates formed in ground waters are due to the presence of vegetable or animal matter. The decomposition of vegetation or animal waste may cause either the oxidation of nitrogen compounds to nitrates or reduction to ammonia. Large amounts of nitrates usually indicate that at some earlier period pollution of considerable extent once existed but has since been oxidized. Any immediate or short connection with surface water or shallow groundwater would falsify the chemical composition of the deep groundwater, and disguise the degree of concentration and the ratios of ions, which are determined by the length of trajectory and the contact of the water with the rock. Therefore, only samples from wells reaching below the level of Lake Simcoe, deeper than 175 feet, and with a nitrate content of less than 12 ppm -- limits which were set rather arbitrarily -- were considered in the evaluation. To illustrate the relationship of the nitrate content with the well depth, average nitrate values of the 30 samples are given:

10 wells less than 200 feet deep:  $\text{NO}_3$  content 14.9 ppm

20 wells deeper than 200 feet:  $\text{NO}_3$  content 2.9 ppm

As already stated, the smaller nitrate content in the deeper wells might have been caused not only by an initial low concentration, but also to some extent by the gradual reduction of  $\text{NO}_3$  in the saturated zone.

The chemical analyses by the Geological Survey of Canada during the groundwater resources survey for different townships in the area (G.S.C. Water Supply Paper Nos. 284, 285, 287, 290, 293, 307, 320) could not be used because of missing nitrate values. For some computations, four water analyses performed by the Ontario Water Resources Commission were used as additional information along the basin divide. The chemical analyses used for calculations are given in Table 1.

The main purpose of the hydrogeochemical study was to reveal any relationship between the location of the water wells and their chemistry, that is, to ascertain if any main groundwater flow directions could be derived. Four main criteria were used for this purpose: concentration, zonation, base exchange, and saturation.

TABLE 1

## Chemical Analysis of Water Samples

Sample No.	57(1)	66(2)	40(4)	21(5)	5(6)	8(8)	129(9)	526(11)
Location Co. Twp. Con. lot	York Markam VI 7	York Markam I 29	York Vaughan VIII 28	York Vaughan VI 6	York Newmarket Yonge St.	York King VII 7	York King o.s. III 16	York Vaughan VIII 16
Distance from basin boundary (in miles)	10.2	11.0	6.0	12.0	5.6	2.4	4.8	9.2
Well depth (in feet)	216	225	290	315	450	487	279	175
Ca ppm epm	50.2 2.5	102 5.1	50.2 2.5	142 7.1	41.5 2.1	52 2.6	31.5 1.6	321 16
Mg ppm epm	6.0 .49	14.6 1.2	8.9 .73	48.9 4.02	18.6 1.5	9.8 .81	13.7 1.13	104 8.6
Na ppm epm	260 11.3	21.2 .92	210 9.1	69.0 3.0	12.8 .56	91.0 4.0	31.0 1.3	568 24.7
K ppm epm	10.3 .26	1.8 .046	9.8 .25	1.6 .041	1.1 .028	2.1 .05	1.6 .04	15.5 .4
HCO <sub>3</sub> ppm epm	183 3.0	304 5.0	345 5.7	209 3.4	241 3.9	310 5.1	222 3.6	218 3.6
SO <sub>4</sub> ppm epm	2.2 .046	46.6 .97	1.7 .035	85.4 1.78	.8 .0002	1.5 .031	1.7 .035	64.4 1.34
Cl ppm epm	400 11.3	53.0 1.5	245 6.9	342 9.6	3.0 .084	87 2.46	13.2 .37	1570 44.3
Sum of above constituents ppm epm	911.7 28.896	543.2 14.736	870.6 25.215	897.9 28.941	318.8 8.1722	553.4 15.051	314.7 8.075	2860.9 98.94
pH	8.0	8.0	8.1	7.4	8.0	7.7	7.8	7.3
s.i. (after Langelier)	+0.4	+0.9	+0.7	+0.3	+0.5	+0.3	+0.1	+0.5
Ca-hardness ppm	150	315	162	556	180	170	135	1230
Specific conductance micro mhos at 25°C	1660	720	1375	1640	400	760	400	5490
Fe ppm	.6	.48	.81	1.8	.69	1.7	.64	1.6
Mn ppm	.1	.16	.02	.22	.02	0.14	.02	.4
NO <sub>3</sub> ppm	.03	.09	.02	.01	.26	4.6	.35	8.5
SiO <sub>2</sub> ppm	8.9	18	9.1	21	22	19.0	23.0	18.0



TABLE 1

## Chemical Analysis of Water Samples (Cont.)

Sample No.	517(12)	531(15)	530(16)	550(17)	553(18)	42(23)	12(24)	11(25)
Location Co. Twp. Con. lot	York Markam V 14	Ontario Reach IX 8	York King III 15	Simcoe Innisfil XII 18	Simcoe Innisfil I 7	York Vaughan X 25	York King o.s. II 18	York King n.s. II 12
Distance from basin boundary (in miles)	8.6	0.8	0.8	5.2	3.6	8.0	6.4	4.8
Well depth (in feet)	230	486	290	486	340	223	370	406
Ca ppm epm	38.8 1.8	35.1 1.6	65.9 3.3	33.7 1.7	10.7 .53	72.6 3.62	35.8 1.8	68.1 3.4
Mg ppm epm	3.1 .25	6.2 .51	13.5 1.1	6.3 .52	.8 .066	34.9 2.9	17.2 1.4	38.9 3.2
Na ppm epm	167 7.26	38.0 1.7	3.1 .13	42.5 1.85	67.5 2.9	29.1 1.3	58.7 2.6	118 5.1
K ppm epm	10.3 .26	2.4 .061	4.8 .12	.9 .023	.4 .01	2.8 .072	2.2 .056	5.5 .14
HCO <sub>3</sub> ppm epm	297 4.87	229 3.8	239 3.9	222 3.64	154 2.5	393 6.4	205 3.4	238 3.9
SO <sub>4</sub> ppm epm	2.3 .048	1.4 .029	22.3 .46	1.6 .033	2.3 .048	46.6 .97	2.2 .046	1.4 .029
Cl ppm epm	180 5.1	2.5 .071	2.1 .059	9.5 .27	37.0 1.04	5.5 .16	76.0 2.14	300 8.5
Sum of above constituents ppm epm	698.5 19.588	314.6 7.771	350.7 9.069	316.5 8.036	272.7 7.094	584.5 15.422	397.1 11.442	769.9 24.269
pH	7.8	7.7	8.0	7.5	7.8	7.8	7.7	7.9
s.i. (after Langelier)	+0.2	+0.1	+0.7	-0.2	-0.6	+0.7	0.0	+0.5
Ca-hardness	102	117	220	110	30.0	325	160	330
Specific conductance micro mhos at 25°C	1100	385	440	400	375	685	570	1350
Fe ppm	1.7	.24	.04	.61	0.2	0.08	.46	1.1
Mn ppm	0.08	.03	0.01	.08	0.01	0.01	.02	0.01
NO <sub>3</sub> ppm	.42	.07	12.0	3.6	.09	0.07	2.2	.09
SiO <sub>2</sub> ppm	10.0	16.0	13.0	17.0	14.0	15.0	20.0	18.0

TABLE 1

## Chemical Analysis of Water Samples (Cont.)

Sample No.	13(26)	14(28)	H(29)	W6117	W3542	W2565	TW 1/69
Location Co. Twp. Con. lot	York King o.s. II 18	Simcoe West Gwillimbury I 2	York Toronto Harwood Park	Ontario Uxbridge Town of Uxbridge	Ontario Uxbridge III 22	York Aurora	York Whitchurch X 15
Distance from basin boundary (in miles)	6.0	2.4	21.2	3.0	1.0	2.6	
well depth (in feet)	286	365	271	251			
Ca ppm epm	35.8 1.8	30.1 1.5	91.4 4.6		39 1.946	32	150
Mg ppm epm	15.9 1.3	12.1 .10	36.9 3.0				
Na ppm epm	55.7 2.4	55.6 2.4	149 6.5				
K ppm epm	2.3 .059	.9 .023	8.5 .22				
HCO <sub>3</sub> ppm epm	207 3.4	279 4.6	269 4.4				
SO <sub>4</sub> ppm epm	3.4 .07	1.5 .031	4.5 .093		15 .312	4 .083	26 .541
Cl ppm epm	73.5 2.07	3.2 .09	365 10.3	3 .084	2 .056	1 .028	2 .056
Sum of above constituents ppm epm	393.6 11.099	382.4 8.744	924.3 29.113	n/ a	n/ a	n/ a	n/ a
pH	7.6	7.4	7.2	7.7	7.8	8.3	8.2
s.i. (after Langelier)	-0.1	-0.3	-0.1				
Ca-hardness ppm	155	132	380	176	198	142	208
Specific conductance micro mhos at 25°C	570	460	1575	285	378		370
Fe ppm	.44	.71	2.4	.22	.24	.35	.15
Mn ppm	0.01	.05	.05				
NO <sub>3</sub> ppm	1.9	.07	3.9	0	.05	.04	0
SiO <sub>2</sub> ppm	21.0	16.0	19.0				

a) Concentration (Conductance, Total Dissolved Solids, Cl-content).

According to the previous investigations it was anticipated that the main recharge area or groundwater divide coincided closely with the basin divide. The electrical conductivity, a very good indicator of the total mineralisation of the groundwater, was plotted versus the distance of the well from the basin divide. This was done separately for the wells of the Lake Simcoe and Lake Ontario basins. In both cases the conductivity increased with the distance from the divide. Although the correlation is not extremely good, the trend seems to be clear (Figure 17). The same diagram was plotted for the chloride content which showed a similar result (Figure 18). To cite Schoeller (1959, p. 68), it should be emphasized that chlorine is one of the most important pointers to the degree of stagnation of a body of groundwater, to its time of contact with the rock, and to the length of its trajectory. Obviously the total concentration of dissolved solids is very closely related to the conductivity and therefore shows the same result.

TABLE 2

Average Concentration Versus Distance from Basin Divide

Distance of well groups from basin divide	Group 1 (10 wells) 6 miles	Group 2 (9 wells) 6 - 21 miles
content of Ca, Mg, Na, K, SO <sub>4</sub> , HCO <sub>3</sub> in ppm in epm	389.3 10.6	900.8 30.1
conductivity in micromhos at 25°C.	554	1,646
Cl - content in epm	1.61	10.1

Table 2 presents the average concentrations of well groups versus their distances from the basin divide. The total dissolved solids and the conductivity in the group 6 - 21 miles from the divide are approximately three times larger than those in the group situated within 6 miles of the divide. The difference in the chloride content, with a factor of 6.3, is even more distinct.

b) Zonation ( $r_{Cl}/r_{HCO_3}$ ,  $r_{SO_4}/r_{HCO_3}$ ,  $r_{SO_4}/r_{Cl}$ ,  $r_{Mg}/r_{Ca}$ ).

The three main interactions between the rock and the groundwater which alter the ratios of the various ions during the water's underground passage are: dissolutions, base exchanges, and reductions. One way to show the ratios of the elements in one type of water, and to compare them with other samples, is the semi-logarithmic graph developed by Schoeller (1962, p. 324). The milli-equivalents of the Ca, Mg, Na+K, Cl, SO<sub>4</sub>, and HCO<sub>3</sub> ions of the 19 samples were plotted in two different groups (Figures 19 and 20). The first group was composed of ten analyses of wells situated within six miles of the basin divide, and the second of nine analyses from wells located 6 to 21 miles from the basin boundary.

Before discussing these chemical relationships, the main lithological features of the quaternary deposits should be recalled. The overburden

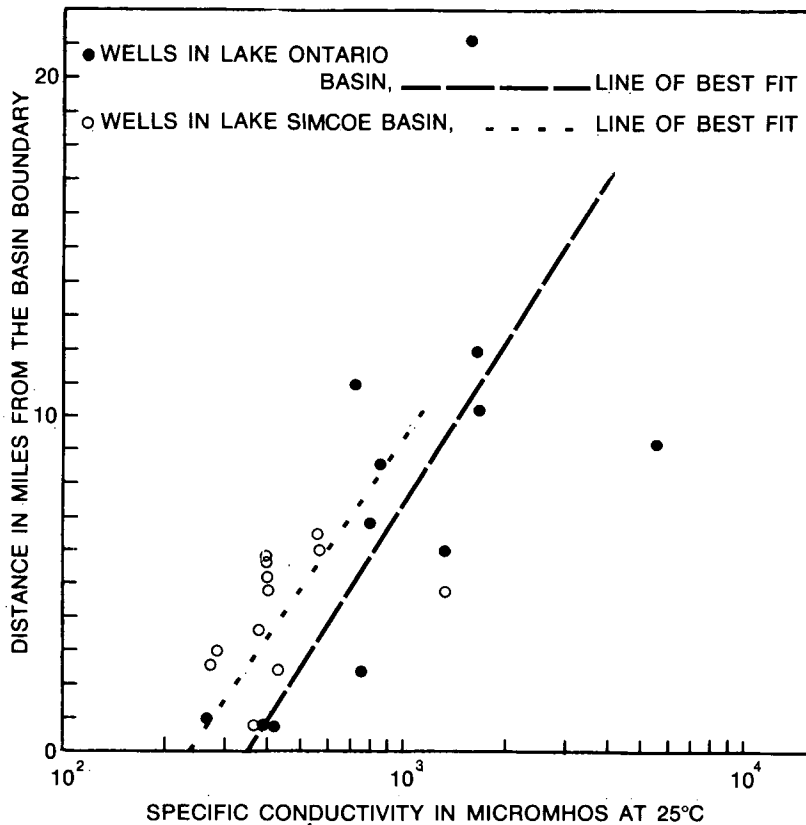
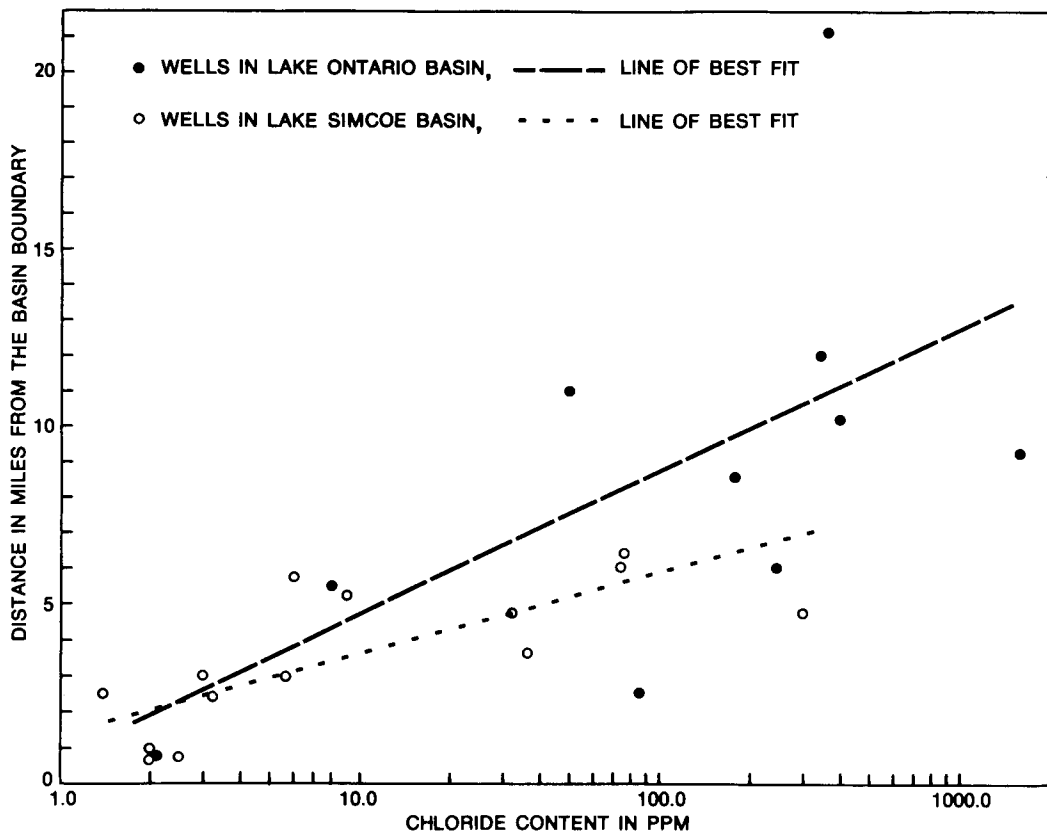


Figure 17. Distance from the basin boundary versus conductivity.

contains no extensive, well defined aquifers. Over 70 percent of the drift consists of till, clay, and hardpan with inserted silt, sand, and gravel lenses. The main groundwater recharge area is situated in the Oakridges moraine region (Plate I). However, due to the nonexistence of region wide, homogeneous, "impermeable" layers, infiltrations into the groundwater body also occur in adjacent areas. Consequently the continuous mineralisation process from the recharge to the discharge area is disturbed. One effect of the disturbance is the scattered distribution of the points in the distance/chloride and distance/conductivity diagrams (Figures 17 and 18).

The relative ratios between the main elements dissolved in the water can be determined directly from the inclination of the connecting lines in the semi-logarithmic plots (Figures 19 and 20). The most obvious difference between the graphs is the previously mentioned, entire mineralisation. It is approximately three times greater in the second group. Both graphs show a certain pattern disrupted by two samples in each - No. 5 and No. 530 in Figure 19 and No. 42 and No. 66 in Figure 20. These four samples have a low Cl and Na+K content, which may indicate a short connection with surface water. To obtain a better picture of the relationship between the elements, the means were computed and included in the graphs. The average values of the



The three different steps are called zones. As Table 3 shows, the wells from the first group represent distinctly the recharge zone 1, and the second group represent zone 2. Although the  $rSO_4/rHCO_3$  ratio is increasing with distance (compare Figures 19 and 20),  $rSO_4$  remains smaller than  $rHCO_3$ ; the pattern of zone 3 has not yet been reached.

TABLE 3

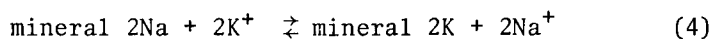
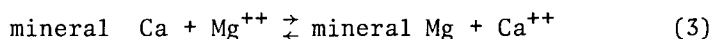
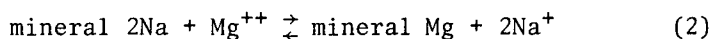
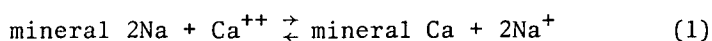
Zonations, Average Ratio Versus Distance from Basin Divide.

Distance of well groups from basin divide	Group 1 (10 wells) 6 miles	Group 2 (9 wells) 6 - 21 miles
$rCl/rHCO_3$	0.41	2.30
$rSO_4/rCl$	0.046	0.059
$rSO_4/rHCO_3$	0.02	0.13
$rMg/rCa$	0.49	0.50

The  $rMg/rCa$  and  $rSO_4/rCl$  ratios can be used for a different type of zonation. However, in this case, there is no significant change between the sample groups. Usually the  $rMg/rCa$  ratio tends to increase towards the discharge area, because the dissolution of  $CaSO_4$  is slower than  $MgSO_4$ , and, after the quick saturation of groundwater in  $CaCO_3$ , not much Ca is dissolved from carbonates. However, more Ca may come into solution from base exchanges, which may disguise the relationship. Since the chlorides have a higher solubility than the sulphates, the  $rSO_4/rCl$  ratio tends to decrease. However, as can be seen from Table 3, the relationships seem to be rather sensitive to base exchanges or secondary infiltrations from the surface.

c) Base Exchange

Groundwater has the ability to exchange cations which are held by minerals, either by the rather weak physical (or Van der Waals) adsorption or by the strong valency bond. With regard to the quaternary deposits of the area, the exchange takes place mainly at the surface of the argillaceous minerals. The following principal exchanges occur (after Schoeller, 1959, p. 63):



The Na/Ca, Na/Mg, Mg/Ca and K/Na ratios change, therefore, with the travel time of the groundwater and might indicate to some extent which exchanges occur. From Table 4, it can be seen that the ratios between the alkalines and the earth alkalines themselves remain constant. If they are exchanged against each other at all it is only to a minor degree. On the other hand, Na increases in relation to Ca and Mg, which would indicate a base exchange as described in equations 1 and 2. However, compared to the earth-alkaline compounds, the higher solubility of the alkaline chlorides

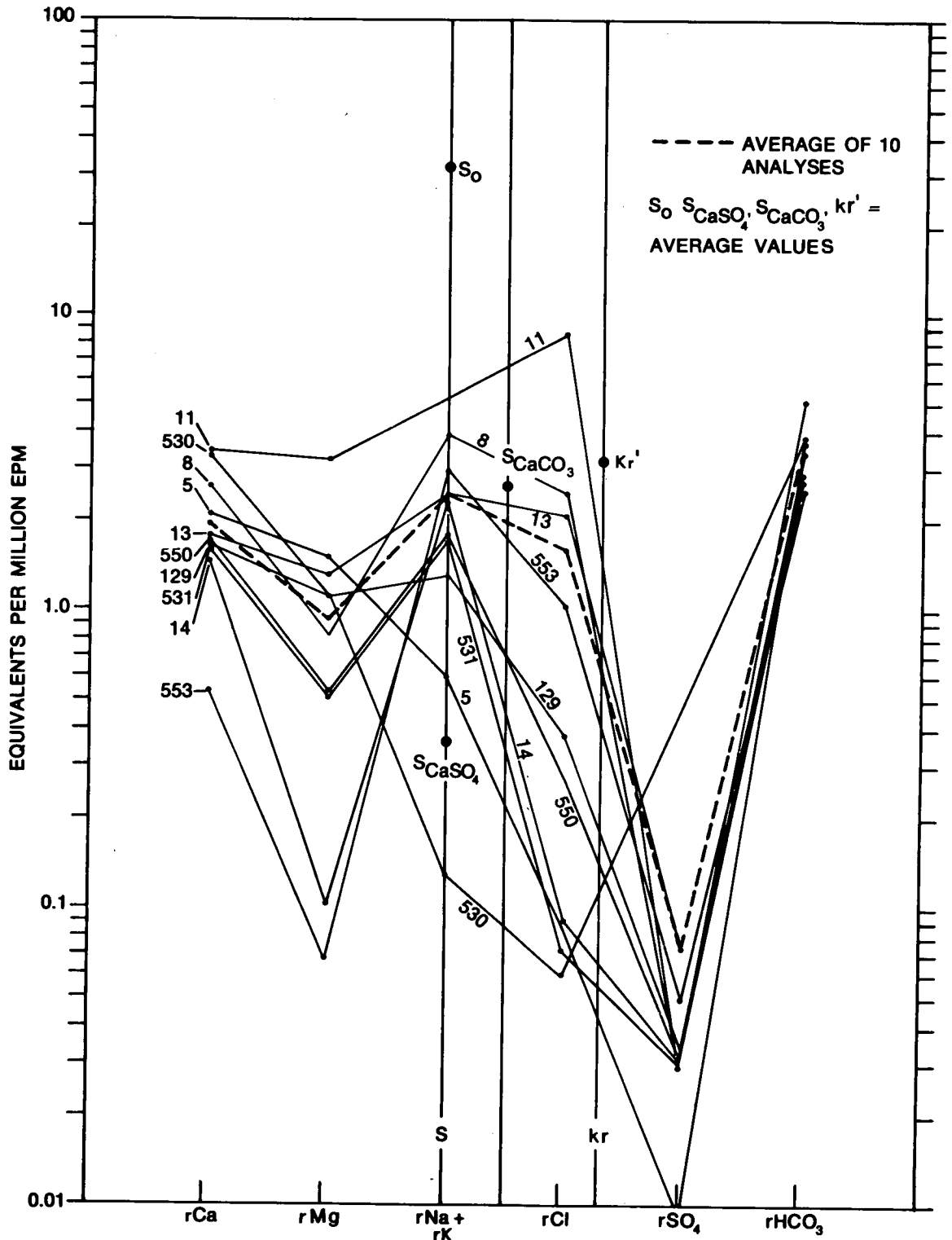


Figure 19. Chemical analysis of group 1: Wells located within 6 miles of the basin divide.

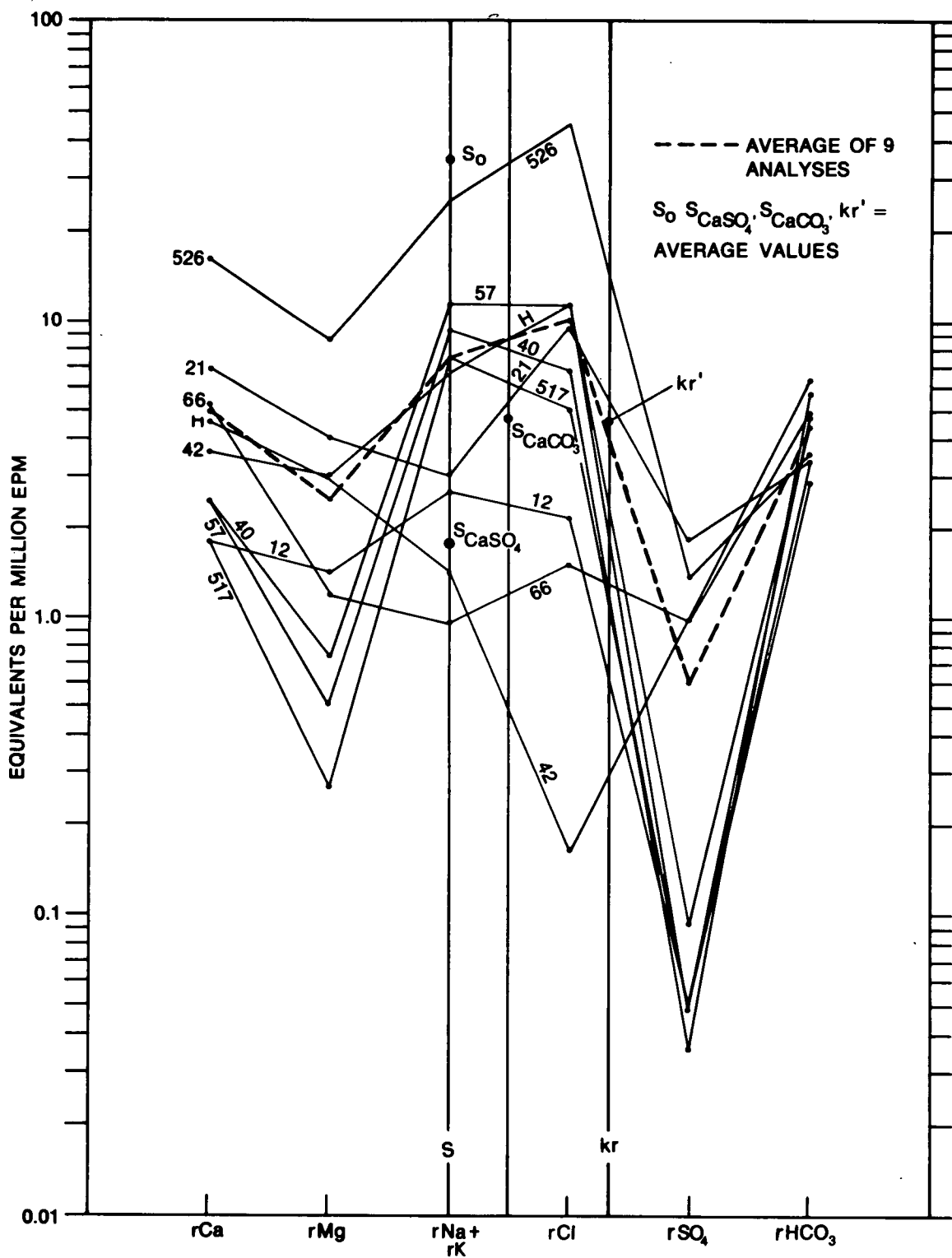


Figure 20. Chemical analysis of group 2: Wells located 6 - 21 miles from the basin divide.



TABLE 4

Base Exchange, Average Ratio Versus Distance from Basin Divide

Distance of well groups from basin divide	Group 1 (10 wells) 6 miles	Group 2 (9 wells) 6 - 21 miles
rNa/rMg	2.57	2.96
rNa/rCa	1.22	1.49
rMg/rCa	0.49	0.51
rK/rNa	0.024	0.023
b.e.i. $(Na^+, K^+) = r \frac{Cl - (Na + K)}{Cl}$	-6.69	-0.76
b.e.i. $(Ca^{2+}, Mg^{2+}) = r \frac{Cl - (Na + K)}{SO_4 + HCO_3 + NO_3}$	-0.43	+0.53
c.r. = $r \frac{Na + K}{Ca + Mg}$	0.85	1.05
a.r. = $r \frac{Cl}{HCO_3 + SO_4}$	0.21	1.09
c.r./a.r.	4.05	0.96

might have a similar cause and possibly change the cation relations. Therefore, in order to determine which base exchanges occur, it becomes necessary to eliminate the dissolution effects. By making two assumptions as follows: (a)  $rCl$  and  $r(Na + K)$  are equal in the original water entering the saturated zone, and (b) all alkalines obtained through the dissolution process are bound to  $Cl$  and the earth-alkalines to the other anions, it becomes possible to determine if any base exchange occurred by comparing both concentrations:

$$rCl - r(Na + K) \quad (5)$$

These assumptions may be invalid in most cases. However, when different samples of the same groundwater stream are compared, it is possible to ascertain if base exchanges occurred and, if so, which ones. The term (5) is then divided by  $rCl$  to obtain a relative value and make comparisons between different samples possible:

$$b.e.i. (Na^+, K^+) = r \frac{Cl - (Na + K)}{Cl} \quad (6)$$

If the alkaline base exchange index, b.e.i.  $(Na^+, K^+)$ , tends to become positive as the water moves downstream, Na and K of the water are exchanged with Mg and Ca of the minerals. If it is negative, the opposite interaction takes place. In the latter case, the term  $r(SO_4 + HCO_3 + NO_3)$  may be introduced as the denominator, as an indication of the amount of earth alkaline obtained through dissolution:

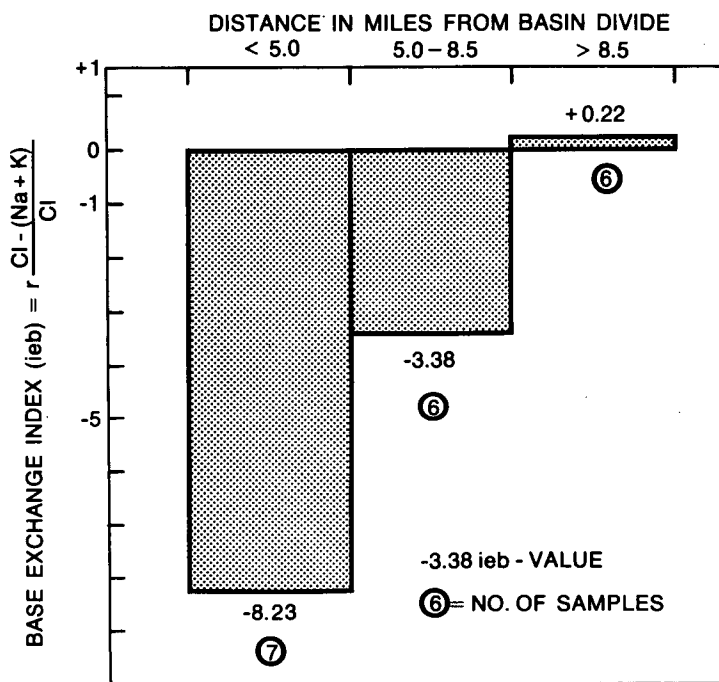
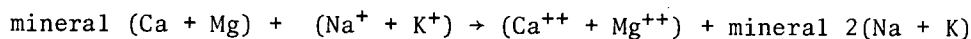


Figure 21. Base exchange index versus distance from basin divide.

$$\text{b.e.i. (Ca}^{++}, \text{Mg}^{++}) = r \frac{\text{Cl} - (\text{Na} + \text{K})}{\text{SO}_4 + \text{HCO}_3 + \text{NO}_3} \quad (7)$$

In the vicinity of the basin divide, both base exchange indices are distinctly negative (Table 4), and tend to become positive with increasing distance, an indication that the exchange



becomes predominant. Figure 21 shows the very clear relationship to the length of the groundwater trajectory.

Another way to reveal the base exchange process is by comparing the anion (a.r.) and cation (c.r.) ratios.

$$\text{a.r.} = r \frac{\text{Cl}}{\text{HCO}_3 + \text{SO}_4} \quad (8)$$

where a.r. is a measure of the alkalines and earth alkalines originating from the dissolution process. Since any possible sulphate reduction is neglected, the denominator represents the minimum amount of dissolved earth alkalines and gives a maximum value for a.r.

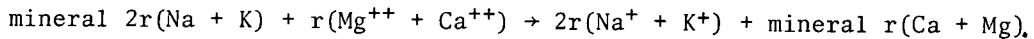
By comparing a.r. with c.r.

$$\text{c.r.} = r \frac{\text{Na} + \text{K}}{\text{Ca} + \text{Mg}} \quad (9)$$

a measure of the magnitude of the base exchange is obtained. If, in the groundwater entering the zone of saturation,  $r(\text{Na} + \text{K})$  is the same as  $r(\text{Ca} + \text{Mg})$ , and  $r\text{Cl}$  the same as  $r(\text{SO}_4 + \text{HCO}_3)$ ,

$$\frac{\text{c.r.}}{\text{a.r.}} > 1$$

would represent



$$\frac{\text{c.r.}}{\text{a.r.}} < 1$$

would represent the opposite reaction. This assumption might seldom be valid because, on its way through the soil, the composition of the water tends to change rapidly. However, by comparing a.r. with c.r. for different water samples from the same groundwater body, it is possible to tell not only the base exchange trend but also its magnitude. By checking groups 1 and 2, (Table 4), the following values of  $r$  are obtained:

$$r_1 = \frac{\text{c.r.}(1)}{\text{a.r.}(1)} = 4.05 \text{ and } r_2 = \frac{\text{c.r.}(2)}{\text{a.r.}(2)} = 0.96.$$

From the recharge versus the discharge zone, it is evident that  $r(\text{Na}^+ + \text{K}^+)$  has been exchanged against mineral  $r(\text{Ca} + \text{Mg})$ . The base exchange reduced the relative alkaline content at least 4.2 times. Since sulphate tends to be reduced as the water moves downstream, causing a.r.(2) to become even smaller, the factor might even be larger. Since the  $\text{NO}_3$  content is extremely small in comparison with the other anions, it has been neglected in the calculations.

d) Saturation of  $\text{CaSO}_4$  and  $\text{CaCO}_3$

Definitions:

$r\text{C}$  = equivalents per million (or epm) of C =

$$\frac{\text{weight in milligrams} \cdot \text{valence}}{\text{formula weight}}$$

$[\text{C}]$  = concentration of C in mol/litre =  $\frac{\text{weight in grams}}{\text{formula weight}}$

$$r\text{C} = 10^3 [\text{C}] \cdot Z_C$$

$\langle \text{C} \rangle$  = activity, applied instead of  $[\text{C}]$ .

$$\langle \text{C} \rangle = \gamma_C \cdot [\text{C}]$$

$$\log \gamma = -0.505 Z^2 \sqrt{\mu}$$

$$\mu = \text{ionic strength} = \frac{1}{2} \sum m_n Z_n^2$$

$$\text{or } \mu = \frac{1}{2} ([\text{C}_1] Z_1^2 + [\text{C}_2] Z_2^2 + \dots + [\text{C}_n] Z_n^2)$$

$$\text{or } \mu = 0.5 \cdot 10^{-3} (rC_1Z_1 + rC_2Z_2 + \dots rC_nZ_n)$$

Z = valence, [C] = m = molality,  $\gamma$  = activity coefficient

The relationship between the ion product,  $S = \sqrt{(rA) \cdot (rB)}$ , used in the Schoeller semi-logarithmic graph method and the corresponding term  $K = [A] \cdot [B]$  is:

$$S = 10^3 \sqrt{Z_A \cdot Z_B \cdot K}$$

Computations: The computation methods are a modified version of those developed by Schoeller (1955).

The ion product of  $\text{CaSO}_4$  is

$$S_{\text{CaSO}_4} = \sqrt{(r\text{Ca}) (r\text{SO}_4)}$$

or  $\log S_{\text{CaSO}_4} = \frac{1}{2} \log (r\text{Ca}) (r\text{SO}_4)$

which is solved graphically with the semi-logarithmic plot (Figures 19 and 20).  $S_{\text{CaSO}_4}$  is halfway along the straight line joining the points  $r\text{SO}_4$  and  $r\text{Ca}$ . To determine how far the water is saturated we compute the solubility product for  $\text{CaSO}_4$ ,  $S_0$ , which depends on  $\mu$  and the temperature  $\theta$ . First, we calculate the ionic strength,  $\mu_{S_0}$ , for the water sample under assumed  $\text{CaSO}_4$  saturation conditions:

$$\mu_{S_0} = 0.062 + (\mu - r\text{CaSO}_4 \cdot 10^{-3})$$

$$0.062 = \mu \text{ for } S_0 \text{ in pure water at } 20^\circ\text{C}$$

and compute the uncorrected solubility product  $S'_0$  from curve a) in Figure 22. The temperature correction factor,  $\alpha$ , is taken from curve b). Since in turn the total temperature correction depends on the value of  $S'_0$ , we compute the actual saturation point,  $S_0$ , after the formula

$$S_0 = S'_0 + \frac{S'_0 \cdot \alpha}{31}$$

$$S_0 = 31 \text{ ppm in pure water at } 20^\circ\text{C}$$

Moving toward the discharge region of our study area the ionic strength,  $\mu$ , and especially  $S_{\text{CaSO}_4}$ , grow rapidly (Table 4).

The dissolution of sulphates increases approximately twice as much as the total mineralisation or the ionic strength. The saturation point,  $S_0$ , is, however, far from being reached.

The pH eq., the pH of the water when saturated with  $\text{CaCO}_3$ , corresponds to the  $\text{CO}_2$  of equilibrium which regulates the equilibrium with the dissolved  $\text{CaCO}_3$ . If the actual pH is less than the pH eq. it means that free  $\text{H}_2\text{CO}_3$  still exists which is not needed to keep the  $\text{CaCO}_3$  in solution:



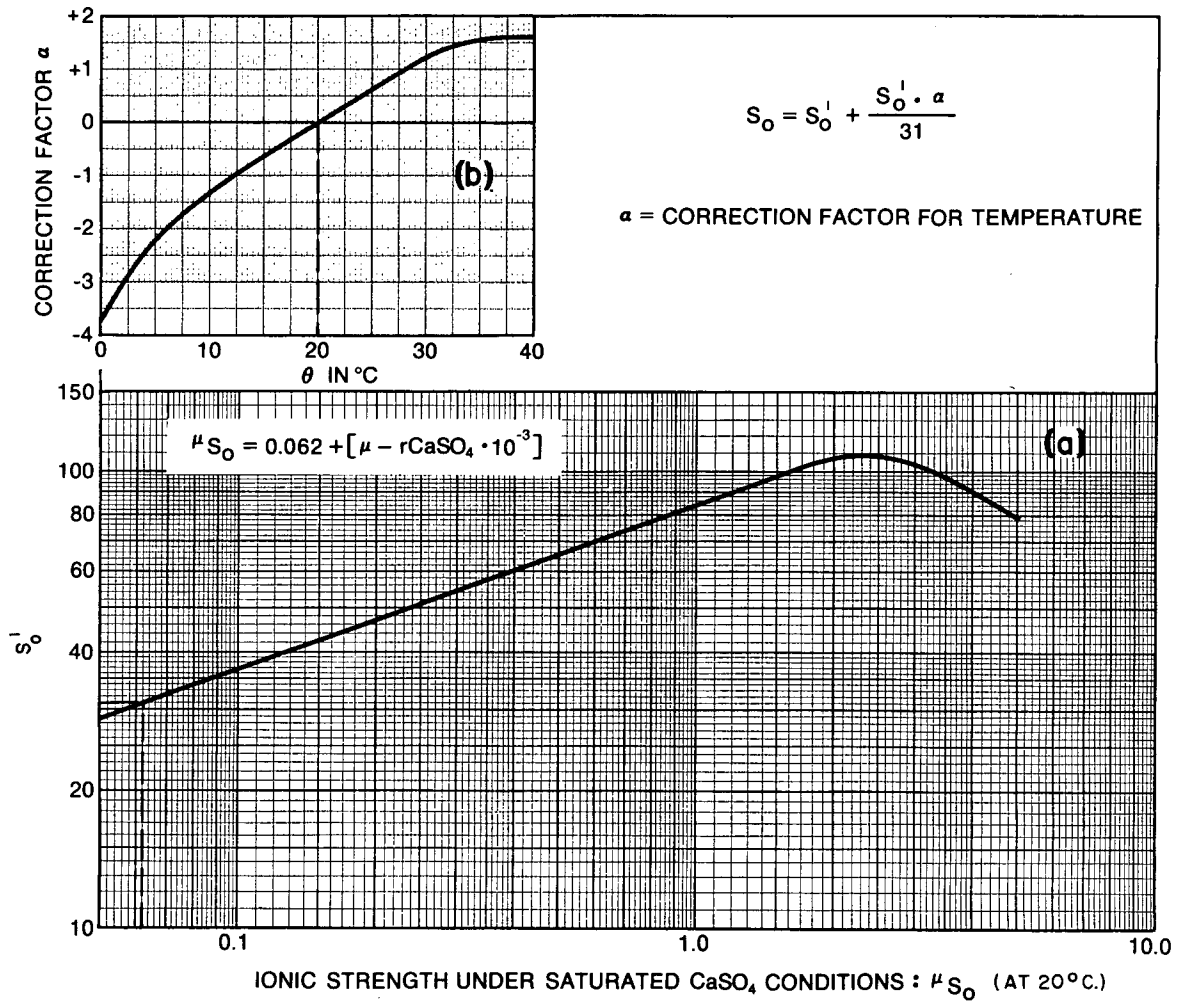
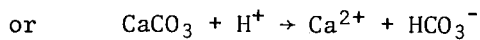
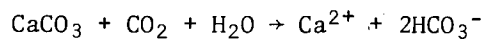


Figure 22. Computation of the saturation point  $S_0$  of  $\text{CaSO}_4$ .

The water in this case is unsaturated in  $\text{CaCO}_3$ , and has an aggressive tendency, especially toward carbonates:



The pH eq. may be computed from the formula

$$S_{\text{CaCO}_3}^2 = 4K_c' \left[ \frac{\langle \text{H}^+ \rangle \text{ eq.}}{2K_2'} + 1 \right]$$

where the equilibrium constants at 25°C are:

$$K_c' = [\text{CO}_3^{2-}] [\text{Ca}^{2+}] = 4.78 \cdot 10^{-(9+4\sqrt{\mu})}$$

$$K_2' = \frac{[H^+][CO_3^{2-}]}{[HCO_3^-]} = 5.61 \cdot 10^{-(11+0.382\sqrt{\mu})}$$

$$(pK_C' = 8.32 - 4\sqrt{\mu}, pK_2' = 10.25 - 0.382\sqrt{\mu})$$

and from the equation

$$S_{CaCO_3} = \sqrt{(rCa)(rHCO_3 + rCO_3)}$$

or  $\log S_{CaSO_4} = \frac{1}{2} \log (rCa)(rHCO_3 + rCO_3)$

$S_{CaCO_3}$  is obtained in the same way as  $S_{CaSO_4}$ ; it is halfway along the straight line joining the points  $rHCO_3$  and  $rCa$  on the semi-logarithmic plot (Figures 19 and 20). For the sake of simplicity, pH eq. is computed directly from Figure 23; after the necessary adjustments have been made for  $\theta$  and  $\mu$ , the corrected pH of equilibrium,  $pH_S$ , is computed. The saturation index, s.i., is negative if the water is unsaturated in  $CaCO_3$  and positive if it is supersaturated. The index may also be calculated after the method of Langelier (1946, p. 169). The values in Table 5, computed after Langelier

TABLE 5

Solubility - and Ion - Product and Saturation Index  
Versus Distance from Basin Divide

Distance of well groups from basin divide	Group 1 (10 wells) 6 miles	Group 2 (9 wells) 6 - 21 miles
$\mu$	$6.78 \cdot 10^{-3}$	$19.08 \cdot 10^{-3}$
$S_{CaSO_4} = \sqrt{(rCa)(rSO_4)}$	0.37	1.75
$\mu_{SO} = 0.062 + (\mu - rCaSO_4 \cdot 10^{-3})$	$66.78 \cdot 10^{-3}$	$75.49 \cdot 10^{-3}$
$S_0'$	31.8	33.0
$S_0 = S_0' + \frac{S_0' +}{31}$ ( $\theta=23^\circ C$ )	32.2	33.4
$S_{CaCO_3} = \sqrt{(rCa)(rHCO_3 + rCO_3)}$	2.7	4.7
pH measured	7.76	7.63
pH eq.	7.37	6.88
$\Delta pH = 3.618 \sqrt{\mu} + \alpha'$ ( $\theta=23^\circ C$ )	0.34	0.55
$pH_S = pH \text{ eq.} + \Delta pH$	7.71	7.43
s.i. = pH - $pH_S$ (after Schoeller)	+0.05	+0.20
s.i. = pH - $pH_S$ (after Langelier)	+0.05	+0.40
$K_R' = \sqrt[3]{(rHCO_3)^2 (rCa)}$	3.05	4.6

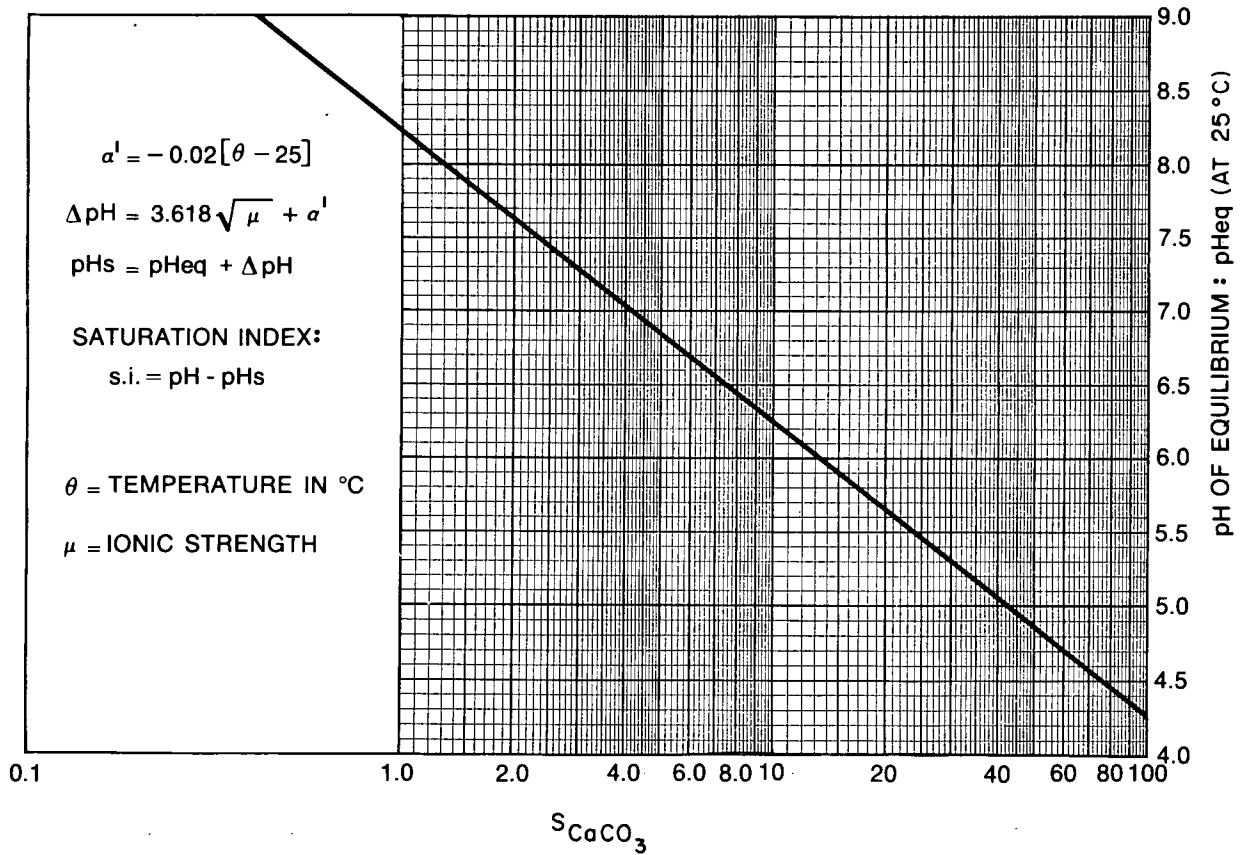


Figure 23. Computation of pH of equilibrium and saturation index.

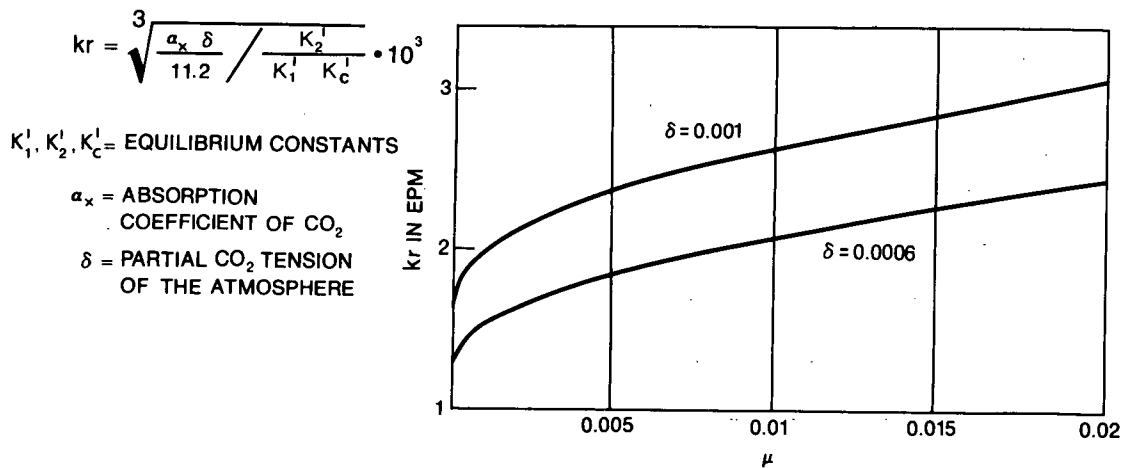


Figure 24. Saturation point of  $\text{CaCO}_3$ ,  $k_r$  as function of the ionic strength (after H. Schoeller: 1962, 279).

and the modified Schoeller method show that the water in the first group is nearly saturated, and in the second group is supersaturated, indicating the expected groundwater flow direction despite the influence of  $\mu$  (see below).

The ion product of  $\text{Ca}(\text{HCO}_3)_2$ ,  $k_R'$ , is computed again in the same manner as the  $S_{\text{CaSO}_4}$ :

$$k_R' = \sqrt[3]{(r\text{HCO}_3)^2 \cdot (r\text{Ca})}$$

or  $\log k_R' = 1/3 \log (r\text{HCO}_3)^2 \cdot (r\text{Ca})$

$k_R'$  is at 1/3 the distance from  $r\text{HCO}_3$  on the straight line joining  $r\text{Ca}$  and  $r\text{HCO}_3$  (Figures 19 and 20). Since the saturation point of  $\text{CaCO}_3$  increases with the ionic strength (valid for  $<1$ ), the groundwater as it moves downstream is able to dissolve more  $\text{CaCO}_3$  without becoming oversaturated (Figure 24). In this case, the well group situated more than 6 miles from the groundwater divide shows an increase in  $k_R'$  of approximately 50 per cent compared with group 1, but only a slight supersaturation (Table 5).

### MATHEMATICAL ANALYSIS

To compute the distribution of the hydraulic potential in the entire groundwater body, and evaluate accordingly the main flow directions in the quaternary deposits, as well as in the bedrock formations, the numerical method developed by Freeze and Witherspoon (1966, 1967, 1968) and Freeze (1969) have been applied. For a better understanding of the investigations, the fundamental definitions and equations on which the mathematical model is based shall be recalled.

The hydraulic head at any given point in a groundwater body is:

$$\phi = \frac{p}{\rho g} + z$$

and the hydraulic potential

$$\Phi = g\phi$$

Darcy's law

$$v_x = k \frac{\delta\phi}{\delta x}$$

$\phi$  = hydraulic head

$\Phi$  = hydraulic potential

$g$  = acceleration due to gravity

$p$  = hydrostatic pressure

$\rho$  = density of water

$z$  = elevation above standard datum

$v_x, v_y, v_z$  = velocities in three coordinate directions

and the equation of continuity for a steady state boundary value problem

$$\frac{\delta v_x}{\delta x} + \frac{\delta v_y}{\delta y} + \frac{\delta v_z}{\delta z} = 0$$

combined, result in Laplace's equation which describes the spatial distribution of the hydraulic head:

$$\frac{\delta^2\phi}{\delta x^2} + \frac{\delta^2\phi}{\delta y^2} + \frac{\delta^2\phi}{\delta z^2} = 0$$



For the elaborate evaluation leading to the numerical analysis of the hydraulic potential in an anisotropic groundwater body and for the computer program, the reader is referred to the Freeze and Witherspoon publications mentioned above.

Based on well records, on test wells drilled in the summer of 1969 for another study, and on the seismic survey by Hobson (1970), two geological cross-sections between Lake Ontario and Lake Simcoe were constructed, (Plate 1). One of them follows coordinate No. 3 from Toronto Harbour to Jacksons Point; the other is constructed along the buried bedrock valley connecting Humber Bay with Cook Bay (Figure 25). Since this is the best defined and deepest channel, it is called the main buried valley. (Although the rather scarce well data east of Woodbridge allow interpretation of the bedrock topography in different ways, the author is rather convinced that the continuation of the Cook Bay channel is the buried valley leading into the Humber Bay and not the one at the Don River (Figure 25). However, since this questionable branching point is about 12 miles south of the basin divide, it doesn't affect the main north-south groundwater flow pattern). Both profiles are 60 miles long, their bottoms are 750 ft. below sea level, and the vertical exaggeration is approximately ten times. Since the study deals with the overall flow pattern of the whole study area, the shape of the water table was generalized and plotted after average piezometric heads measured in deep wells. Therefore it does not reflect local conditions produced by hummocks or river valleys.

The permeability of the different formations, the other important factor controlling groundwater flow, was computed or estimated in the following manner - the average specific capacity,  $Q/s$ , of the overburden was converted into an approximate transmissibility value,  $T$ , after Meyer (1963, p. 338). In order to obtain a general average permeability for the quaternary deposits,  $T$  was divided by the average length of the wells below water level. Due to the predominant horizontal flow to a discharging well, the permeability obtained from a pumping test represents the one in the horizontal direction,  $K_h$ . Since any quaternary deposit is anisotropic, the permeability in the vertical direction,  $K_v$ , is different from  $K_h$ . It is necessary to distinguish between the anisotropy of a single homogeneous bed and the anisotropy resulting from the stratification. The first is measurable in core samples, the second, and more important one, can be evaluated by pumping tests using either partially penetrating wells (Weeks, 1969, p. 196) or wells in leaky aquifers (Walton, 1960). Since not enough of the required data were available, the  $K_v$  values were estimated, mainly after a literature review (Freeze, 1969; Norris, 1962; Walton, 1965; and others). The  $K_h/K_v$  ratio, being of great importance for quantitative problems, was of less significance for this qualitative study, since the author was only interested in locating the groundwater divide in the different formations, and in obtaining the main recharge and discharge areas. The permeability of the Trenton and Black River Group limestone was computed in the same way as that of the overburden, but it had to be assumed from values applicable outside the area (Chapter 2). In addition, the generally decreasing fracture porosity with depth had to be given some consideration (Snow, 1968, p. 73). It is believed that the resulting  $K$  factor of approximately  $1.0 \text{ Igpd/ft}^2$  was rather on the high side. Furthermore, the assumption was made that the  $\pm$  vertical fracture system and the horizontal bedding control the groundwater flow equally, thus giving  $K_h = K_v$ . For the less important shale formations and for the crystalline rocks, rather arbitrary empirical values were taken for  $K$ . For the sake of simplicity all permeability values vary by a factor of ten.

Plate I shows the distribution of the equipotential lines and the main groundwater flow directions in both north-south oriented profiles. The equipotential lines were taken from computer plots, and the general direction of flow was plotted accordingly. Both cross sections in all layers show a well defined groundwater divide coinciding with the basin boundary. The same profiles were also computed with  $K_v = 1.0$  and  $0.2$  for the overburden, without a distinct effect on the general flow pattern.

To show under which situation major seepage might occur from the Lake Simcoe basin across the surface water divide into Lake Ontario, different hypothetical hydrogeologic conditions of the quaternary deposits were simulated. Two different layers with very unlike permeabilities were introduced. The top layer might represent a clay or a very dense till, whereas the second bed consists of a clean sand and gravel aquifer (Plate II). Under these conditions the shape of the water table reduces its influence, and the difference in elevation between Lake Simcoe and Lake Ontario becomes more important. Due to the distinctive stratification, the horizontal flow becomes predominant. Under the conditions of case a) the groundwater divide in the deeper layers is shifted five miles toward Lake Simcoe. By increasing  $K_h$  for both assumed overburden layers by a factor of 10, case b), magnifying the anisotropy even more, the divide is moved so far north that we obtain a distinct groundwater flow from Lake Simcoe into Lake Ontario.

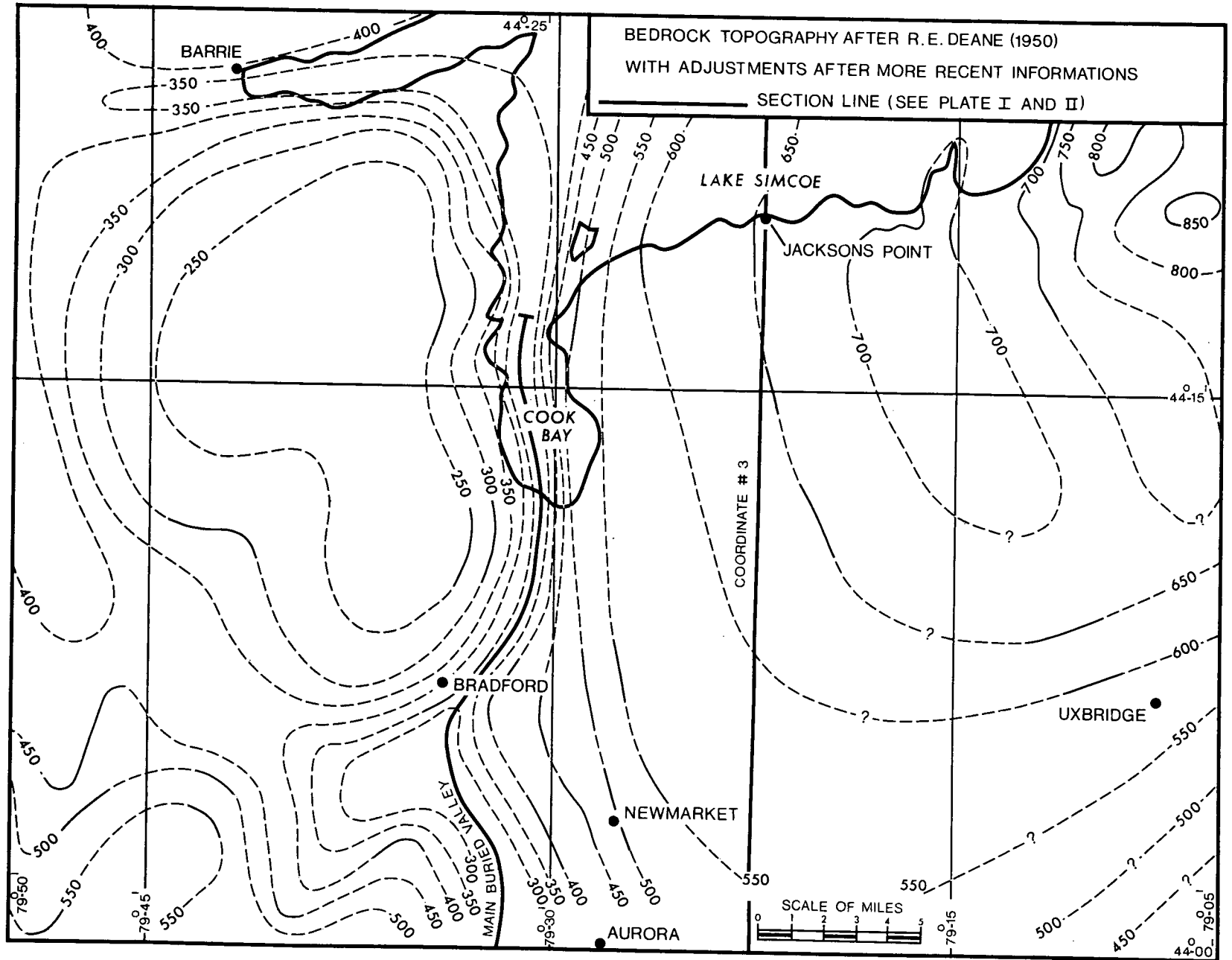


Figure 25 (Sheet 1). Bedrock topography between Lake Simcoe and Lake Ontario (with contribution from G.D. Hobson, Geol. Surv. of Canada).

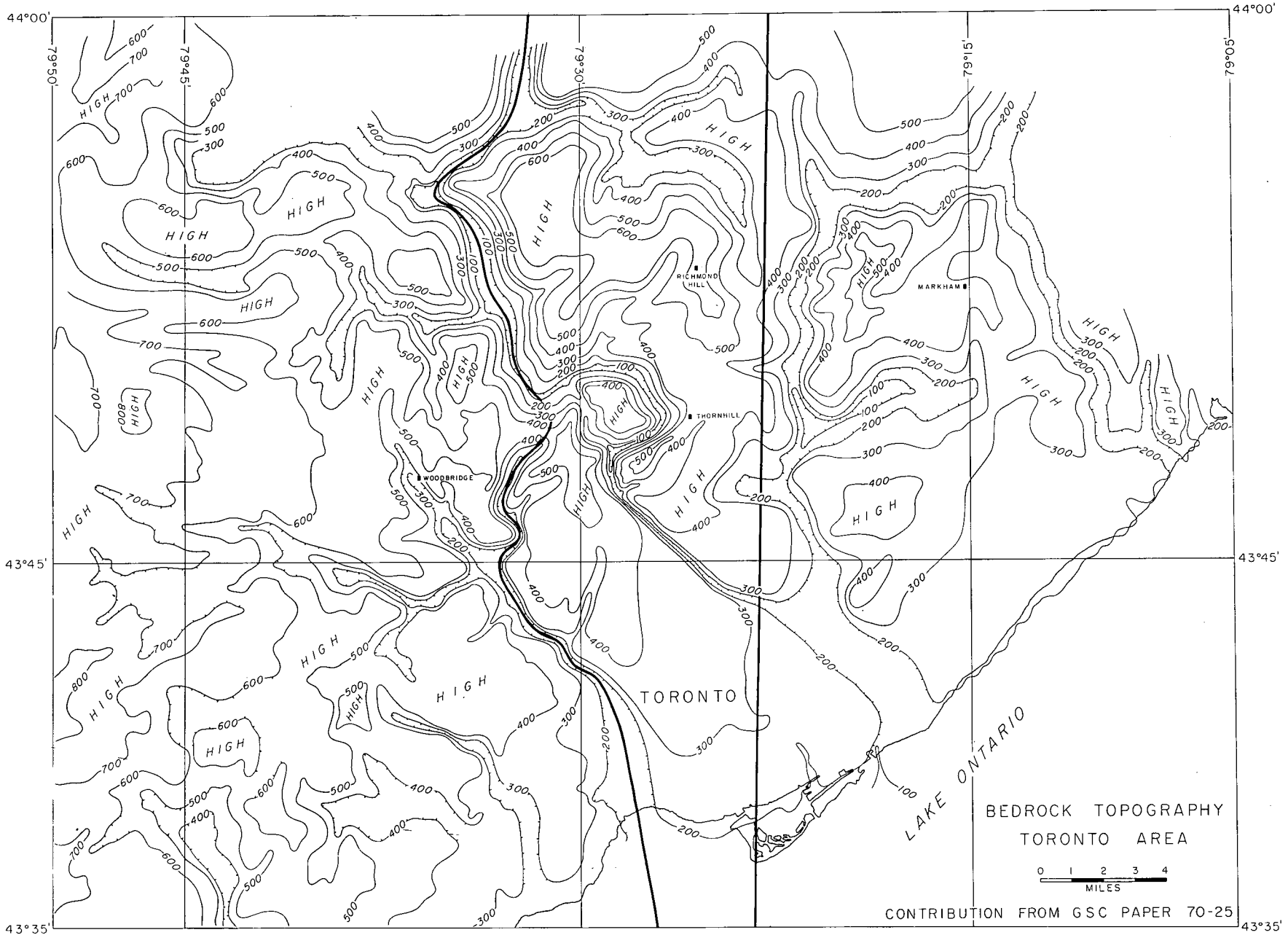


Figure 25 (Sheet 2). Bedrock topography between Lake Simcoe and Lake Ontario (with contribution from G.D. Hobson, Geol. Surv. of Canada).

## *Conclusions*

1. The thickness of the quaternary deposits varies considerably between Lake Ontario and Lake Simcoe. Apart from the well defined bedrock channels which are covered by up to 700 feet of overburden the following trend can be observed. From less than 50 feet at the south-eastern shore of Lake Simcoe, the drift increases to over 400 feet in the area between Newmarket and Richmond Hill. From there, it begins to decrease southwards, becoming 25 to 75 feet thick along Lake Ontario's shoreline south and west of Toronto. An east-west section shows the largest accumulation in the central part, a distinct decrease to 150 feet or less in the area of Woodbridge, and a variable thickness around Markham of 100 to 250 feet.
2. Regional, extensive, well defined aquifers do not exist. The general pattern of the quaternary deposits is a body of very low permeability with enclosed high permeable lenses of various sizes.
3. The average specific capacity of 217 wells deeper than 200 feet spread over the whole region is 1.1 Igpm/ft, and for 88 wells deeper than 200 feet, situated in the main channel area, is 0.5 Igpm/ft. The permeability generally decreases with the channel depth. The overall mean permeability of the entire quaternary deposits is about 10 Igpd/ft<sup>2</sup>. The highest transmissibility values for the most productive aquifer lenses ranges approximately from 40,000 to 80,000 Igpd/ft which suggests that good aquifers do exist although they may be difficult to define. Most of the pumping tests show impermeable boundary conditions.
4. The configuration of the water table corresponds generally with the topography. Piezometric, hydrogeochemical and mathematical analyses demonstrate the non-existence of major seepage from Lake Simcoe into the Lake Ontario basin. The groundwater divide coincides approximately with the basin boundary in the quaternary deposits as well as in the different underlying bedrock formations.
5. The following hydrochemical criteria were found to be particularly useful to determine the groundwater flow direction: total mineralisation, electrical conductivity, Cl content, rCl/rHCO<sub>3</sub>, rSO<sub>4</sub>/rHCO<sub>3</sub>, base exchange indices, cation/anion ratio, concentration of CaSO<sub>4</sub> and CaCO<sub>3</sub>.
6. The numerical method developed by Freeze and Witherspoon proved to be an extremely valuable tool to analyse regional groundwater flow problems, especially in deep bedrock formations with very little existing data, and for the simulation of various hydrogeological conditions.

## References

- Back, W. 1961. Calcium Carbonate Saturation in Groundwater from Routine Analyses. U.S. Geol. Survey, Water Supply Paper 1535-D.
- Beards, R.S. 1967. Guide to the Subsurface Palaeozoic Stratigraphy of Southern Ontario. Ont. Dept. of Energy and Resources Management Paper 67-2.
- Chapman, L.J. and D.F. Putnam. 1943. The Moraines of Southern Ontario. Trans. Roy. Soc. of Can., Sect. IV, p. 3.
- Chapman, L.J. and D.F. Putnam. 1943. The Physiography of Southern Ontario. Sci. Agriculture, Nov. 1943, 24, 3.
- Chapman, L.J. and D.F. Putnam. 1949. The Recession of the Wisconsin Glacier in Southern Ontario. Trans. Roy. Soc. of Can., Vol. XLIII, Ser. III, Sect. IV, p. 23.
- Chapman, L.J. and D.F. Putnam. 1966. The Physiography of Southern Ontario. Ont. Res. Found., Univ. of Toronto Press, 2nd ed.
- Charron, J.E. 1969. Hydrochemical Interpretation of Groundwater Movement in the Red River Valley, Manitoba. Sci. Ser. No. 2, Inland Waters Branch, Dept. of Energy, Mines and Resources, Ottawa.
- Chebotarev, I.I. 1955. Metamorphism of Natural Waters in the Crust of Weathering. I. Geochimica et Cosmochimica Acta., Vol. 8, p. 22-48. Permagon Press, London.
- Chebotarev, I.I. 1955. Metamorphism of Natural Waters in the Crust of Weathering. II. Geochimica et Cosmochimica Acta., Vol. 8, p. 137-170. Permagon Press, London.
- Chebotarev, I.I. 1955. Metamorphism of Natural Waters in the Crust of Weathering. III. Geochimica et Cosmochimica Acta., Vol. 8, p. 198-212. Permagon Press, London.
- Deane, R.E. 1950. Pleistocene Geology of the Lake Simcoe District, Ontario. G.S.C. Memoir 256.
- Department of Energy Resources of Ontario, Toronto. Well records from microfilm, 1880-1962.
- Department of Energy Resources of Ontario, 1963. Annual Report, Toronto, 1963.
- Freeze, R.A. 1969. Hydrology and Groundwater Resources of the Gravelbourg Aquifer, Saskatchewan. Sci. Ser. No. 6, Inland Waters Branch, Dept. of Energy, Mines and Resources, Ottawa.
- Freeze, R.A. 1969. Hydrology of the Good Spirit Lake Drainage Basin, Saskatchewan. Tech. Bull. No. 14, Inland Waters Branch, Dept. of Energy, Mines and Resources, Ottawa.
- Freeze, R.A. 1969. Theoretical Analysis of Regional Groundwater Flow. Sci. Ser. No. 3, Inland Waters Branch, Dept. of Energy, Mines and Resources, Ottawa.

REFERENCES (Cont.)

- Freeze, R.A. and P.A. Witherspoon. 1966. Theoretical Analysis of Regional Groundwater Flow. I. Analytical and Numerical Solutions to the Mathematical Model. Water Resources Research, Vol. 2, No. 4.
- Freeze, R.A., and P.A. Witherspoon. 1967. Theoretical Analysis of Regional Groundwater Flow. II. Effect of Water-table Configuration and Sub-Surface Permeability Variation. Water Resources Research, Vol. 3, No. 4.
- Freeze, R.A. and P.A. Witherspoon. 1968. Theoretical Analysis of Regional Groundwater Flow. III. Quantitative Interpretations. Water Resources Research, Vol. 4, No. 3.
- Geological Survey of Canada: Water Supply Papers: No. 284 (1947), 285 (1947), 287 (1948), 290 (1948), 293 (1948), 307 (1950), 320 (1952).
- Gravenor, C.P. 1957. Surficial Geology of the Lindsay-Peterborough Area; Ontario, Victoria, Peterborough, Durham, and Northumberland Counties, Ontario. G.S.C. Memoir 288.
- Guidebook-Geology of Central Ontario. 1964. Amer. Ass'n of Pet. Geol., and The Soc. of Econ. Paleontologists and Mineralogists.
- Hewitt, D.F. 1966. Geological Notes for Map 2117., Geol. Circ. 15, Ont. Dept. of Mines, Toronto.
- Hobson, G.D. 1970. Bedrock Topography of an area North of and including Metro Toronto. G.S.C. Paper 70-25. (In press).
- Karrow, P.F., J.R. Clarke, and J. Terasmae. 1961. The Age of Lake Iroquois and Lake Ontario. J. Geol., Vol. 69, No. 6.
- Karrow, P.F. 1964. Pleistocene Geology of the Thornhill Area. Preliminary Geological Map No. p. 244., Ont. Dept. of Mines, Toronto.
- Langelier, W.F. 1946. Chemical Equilibria in Water Treatment. J.A.W.W.A., Vol. 38.
- Liberty, B.A. 1953. Preliminary Map, Alliston; Simcoe, York and Dufferin Counties, Ontario. G.S.C. Paper 53-9.
- Liberty, B.A. 1953. Preliminary Map, Newmarket; Ontario and York Counties, Ontario. G.S.C. Paper 53-2.
- Liberty, B.A. 1953. Preliminary Map, Oshawa; Ontario and Durham Counties, Ontario. G.S.C. Paper 53-18.
- Liberty, B.A. 1960. Rice Lake, Port Hope and Trenton Map Areas, Ontario. G.S.C. Paper 60-14.
- Liberty, B.A. 1969. Palaeozoic Geology of the Lake Simcoe Area, Ontario. G.S.C. Memoir 355.
- Meyboom, P. 1966. Current Trends in Hydrology. Earth Sci. Rev., Vol. 2, p. 345-364. Elsevier, Amsterdam.

#### REFERENCES (Cont.)

- Meyer, R.R. 1963. *In* Bentall, R. (compiler); Methods of Determining Permeability, Transmissibility, and Drawdown. U.S. Geol. Survey Water Supply Paper 1536-I.
- Norris, S.E. 1962. Permeability of Glacial Till. U.S. Geol. Survey Res. 1962.
- Ontario Dept. of Mines. Ground Water Bulletins: No. 145 (1953) for 1948, 1949, 1950; No. 152 (1957) for 1951, 1952. Toronto.
- Ontario Dept. of Mines. Preliminary Geological Map No. p. 236. 1964. Pleistocene Geology of the Woodbridge Area; York County, Ontario.
- Ontario Water Resources Commission. Ground Water Bulletins: No. 1 (1961) for 1953, 1954; No. 2 (1963) for 1955, 1956; No. 3 (1965) for 1957; No. 4 (1966) for 1958; No. 5 (1966) for 1959. Toronto.
- Rogers, D.P., R.C. Ostry, and P.F. Karrow. 1961. Metropolitan Toronto Bedrock Contours. Preliminary Map 102, Ont. Dept. of Mines, Toronto.
- Sanford, B.V. 1969. Map 1263A: Geology of the Toronto-Windsor Area, Ontario. G.S.C.
- Schoeller, H. 1955. Géochimie des Eaux Souterraines, Applications aux Eaux des Gisements de Petrole. Rev. de l'Inst. franc. Petrole, Vol. II, pp. 181-213; 219-246; 507-552; 671-719; 823-874.
- Schoeller, H. 1959. Arid Zone Hydrology - Recent Developments. Arid Zone Research - XII, Unesco.
- Schoeller, H. 1961. l'Interprétation des Analyses Chimiques des Eaux Salées. Arid Zone Research Vol. XIV. Unesco.
- Schoeller, H. 1962. Les Eaux Souterraines. Masson & Cie, Paris.
- Snow, D.T. 1968. Rock Fracture Spacings, Openings and Porosities. J. Soil Mech. and Found. Div., Amer. Soc. Civ. Eng. Proc. Jan. 1968, p. 73.
- Thomas, J.F.J. 1953. Scope, Procedure and Interpretation of Survey Studies. Industrial Wat. Research of Can., Water Survey Report No. 1. Dept. of Mines and Tech. Surveys, Ottawa.
- Todd, D.K. 1959. Ground Water Hydrology. John Wiley and Sons Inc., New York.
- Walton, W.C. 1960. Leaky Artesian Aquifer Conditions in Illinois. Ill., State Water Survey Report of Investigation 39.
- Walton, W.C. 1965. Ground Water Recharge and Runoff in Illinois. Ill., State Water Survey Report of Investigation 48.
- Watt, A.K. 1957. Pleistocene Geology and Ground Water Resources of the Township of North York and York County. Report of Ont. Dept. of Mines, Vol. LXIV, Part 7.



REFERENCES (Cont.)

Week, E.P. 1969. Determining the Ratio of Horizontal to Vertical Permeability by Aquifer Test Analysis. Water Resources Research, Vol. 5, No. 1, p. 196.

TECHNICAL BULLETIN SERIES

- No. 12 Sediment surveys in Canada. W. Stichling and T.F. Smith, 1969.  
*An outline of the Sediment Survey Program of the Water Survey of Canada, including methods, instrumentation and data available.*
- No. 13 Climatology studies of Baffin Island, Northwest Territories. R.G. Barry and S. Fogarasi, 1969.  
*A report of the results of a program of climatological investigations in Baffin Island.*
- No. 14 Hydrology of the Good Spirit Lake Drainage Basin, Saskatchewan: A preliminary analysis. R.A. Freeze, 1969.  
*A report on the first water balance for the Good Spirit Lake Drainage Basin and a discussion of the methods used in the investigations.*
- No. 15 Digitizing hydrographs and barographs. T.W. Maxim and J.A. Gilliland, 1969.  
*A discussion of the conversion of analogue water level recorder graphs and barographs to digital form using a pencil follower and key punch.*
- No. 16 The computation and interpretation of the power spectra of water quality data. A. Demayo, 1969.  
*A discussion of the concept of spectral analysis and the method of calculating power spectra of water quality data, including a practical example and the computer program used to perform this type of calculation.*
- No. 17 Groundwater Investigation - Mount Kobau, British Columbia. E.C. Halstead, 1969.  
*A report of the results obtained from a study of the groundwater storage system at the summit of Mount Kobau, British Columbia.*
- No. 18 The effects of the W.A.C. Bennett Dam on downstream levels and flows. A. Coulson and R.J. Adamcyk, 1969.  
*A report summarizing the expected effects of the W.A.C. Bennett Dam on levels and flows in the Mackenzie River basin.*
- No. 19 Airborne techniques in climatology; oasis effects above prairie surface features. R.M. Holmes, 1970.  
*A report describing a pilot study of oasis effects in southern Alberta using a specially-instrumented aircraft and a mobile ground station.*
- No. 20 Hydrogeological Reconnaissance of the North Nashwaaksis River Basin, New Brunswick. J.E. Charron, 1969.  
*A description of a hydrogeological reconnaissance carried out as part of an International Hydrological Decade study of the hydrology of the North Nashwaaksis Basin.*
- No. 21 An instrumented experimental site for the investigation of soil moisture, frost, and groundwater discharge. R.A. Freeze and J.A. Banner, 1970.  
*A report describing an instrumented experimental site at Calgary, Alberta, to provide integrated measurements of the subsurface moisture regime in saturated and unsaturated zones. A summary of the first year's operation is included.*
- No. 22 Detergents, phosphates and water pollution. W.J. Traversy, P.D. Goulden and G. Kerr, 1970.  
*A report on the results of chemical analyses of phosphate content in detergents and washing products. The report traces the development of washing products from organic soaps to modern phosphate-based detergents and describes the relationship between phosphates and the eutrophication process.*

A complete list of titles in the Technical Bulletin Series and copies of any of these publications may be obtained from the Director, Inland Waters Branch, Department of Energy, Mines and Resources, Ottawa, Ontario.

Plate I. Hydrogeological cross sections between Lake Simcoe and Lake Ontario.

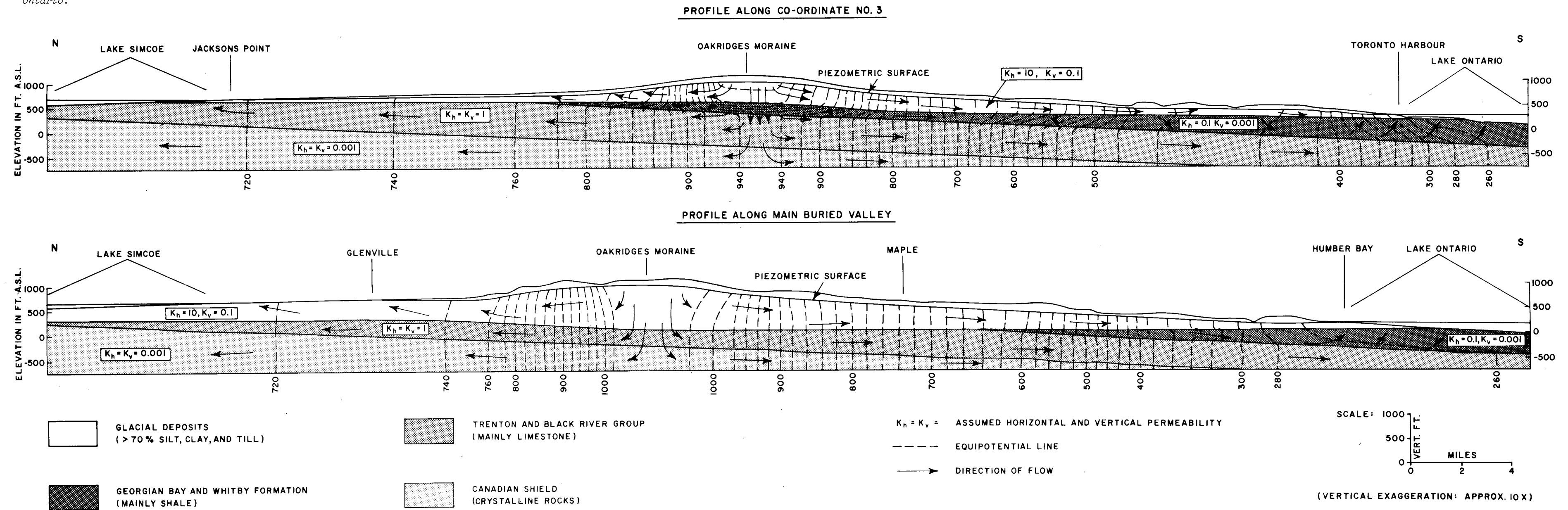


Plate II. Simulated groundwater flow between Lake Simcoe and Lake Ontario.

